Main Manuscript for

Snakes (*Erythrolamprus* spp.) with a complex toxic diet show convergent yet highly heterogeneous voltage-gated sodium channel evolution

Valeria Ramírez-Castañeda[1,2],*; Rebecca D. Tarvin[1]; Roberto Marquéz[3]

[1]Museum of Vertebrate Zoology and Department of Integrative Biology, University of California, Berkeley, CA, 94720

[2]Department of Biological Sciences, Universidad de los Andes, Bogotá, AA 4976, Colombia

[3]Department of Biological Sciences, Virginia Tech, Blacksburg, VA 24060

*Valeria Ramírez-Castañeda

Email: vramirezc@berkeley.edu

Author Contributions:

Design of the work VRC, RM

Acquisition of data VRC

Data analysis VRC

Interpretation of data VRC, RDT, RM

First draft VRC

Revisions VRC, RDT, RM

Competing Interest Statement: Disclose any competing interests here.

Classification: Paste the major and minor classification here. Dual classifications are permitted, but cannot be within the same major classification.

Keywords: Toxin resistance, Voltage-Gated Sodium Channels, *Erythrolamprus* snakes, poison frogs, Tetrodotoxin

This PDF file includes:

Main Text
Figures 1 to 5

Abstract

Chemical defenses shape ecosystems by orchestrating interactions between species and promoting specialization on toxic prey. Many toxins exist in highly biodiverse tropical ecosystems,

sometimes in the same prey, imposing challenges for studying toxin resistance and requiring the development of new models. Royal ground snakes (*Erythrolamprus*) play a significant but understudied role as predators of poisonous frogs (Bufonidae, Dendrobatidae). Several frog toxins affect the voltage-gated sodium channels (VGSCs) and sodium potassium pumps; resistance can evolve in these genes through mutations in target sites, known as target-site resistance (TSR). We investigated potential TSR in VGSC orthologs and traced their phylogenetic origin and geographic presence in six *Erythrolamprus* species and 15 snake outgroups from Colombia. We reveal convergent evolution of TSR in VGSCs of three *Erythrolamprus* snake species: *E. epinephelus*, *E. reginae*, and *E.* sp. We found nine sites in the VGSC pore at which neurotoxin-resistance-related amino acid changes occur in eight VGSC genes, suggesting coordinated evolution of this gene family. Amino acid substitutions at four of these positions were previously reported as conferring tetrodotoxin resistance in other species, however, the dietary source of tetrodotoxin in these snake species is unclear. Across genes, species, and populations, these sites exhibit high heterogeneity of alleles, suggestive of an evolutionary dynamic that maintains polymorphisms, such as balancing selection. These findings provide insight into the evolution of predators with a complex toxic diet, paving the way for new research models to address complex coevolutionary questions in exceptionally diverse tropical ecosystems.

Significance Statement

This study introduces a new evolutionary model in highly biodiverse and chemically diverse ecosystems where prey with multiple toxins and their predators interact. We show convergent origins of protein variants that confer toxin resistance in three species of Royal Ground snakes (*Erythrolamprus* spp.) in the Colombian tropics. We found high variation in toxin-resistant protein variants within and among individuals, species, and populations of snakes, possibly because of their wide geographical and ecological range. Variation in available toxic prey likely trades off with the impact of toxin resistance on protein function, resulting in diversity in adaptations to toxic prey; thus, diversity begets diversity.

Main Text

Introduction

Chemical defense is an anti-predatory trait spread widely throughout the network of life. Along with chemical defenses evolves the ability to resist them, both in the organisms defending themselves (e.g., prey) and those that they target (e.g., predators). Three molecular resistance mechanisms have been proposed to counteract exposure to toxins, 1) detoxifying or clearing the toxin, 2) expressing toxin-binding proteins or transporters that prevent the toxin from reaching its target site, and 3) evolving insensitivity in the proteins that are targeted by the toxin, a mechanism called target-site resistance (TSR) (1–8). TSR appears to be an especially common or more easily quantified adaptation (see references in (9)). For example, a wide variety of animals present a suite of convergent mutations in voltage-gated sodium channels (VGSCs), many of which have been shown to confer tetrodotoxin (TTX) resistance *in vitro* (10–13). Other amino acid substitutions in a nicotinic acetylcholine receptor encode TSR for epibatidine (3), and mutations in the sodium-potassium ATPase pump counteract cardiotonic steroids (14, 15). The recurrent origin of similar or the same amino acid substitutions in the presence of toxins has shown to be molecularly constrained, thus often resulting in biased convergent adaptations, as coined by Agrawal (16). The widespread convergence in TSR suggests that screening DNA sequences is a

powerful tool to investigate possible toxin-resistance mechanisms in previously unstudied taxa (11).

Convergent adaptations have been categorized by their underlying mechanisms (16). For example, in unbiased convergent adaptations, the phenotype is equally likely to be produced by distinct molecular mechanisms, while in biased convergent adaptations some mechanisms are more likely than others, often resulting in convergent phenotypes produced by shared molecular mechanisms (16). Fine-scale variation in biased convergent adaptations could be used to trace microevolutionary processes because the allele diversity and frequency tend to be less extensive than in unbiased convergent adaptations. However, the specificity of a shared molecular mechanism in a biased convergence could vary, for example, increased affinity for oxygen can be conferred by substitutions in different sites of the same protein (17), or in the case of several TSR mechanisms that exhibit a simple genetic basis, different sets of amino acid changes or different amino acid substitutions at the same site could lead to the same or similar TSR phenotype (see references in (9)). Thus, the same phenotype can be produced by fine-scale variations in the genotype, which could be fixed or could vary within species and populations (e.g., (11, 18, 19)). Although there are numerous examples of convergent evolution of TSR, there is less evidence regarding how microevolutionary processes such as population structure or ecology and community composition condition the evolution of the convergent phenotype. For example, molecular variants could appear between populations because of relaxation of selection, exposure to different natural selection regimes, population-based historical contingencies, or changes in population demography, among others, providing opportunities to explore processes underlying population-level biodiversity and its potential role in speciation and ecosystem change (16).

The coexistence of multiple toxins at several trophic levels is common in ecologically and chemically complex ecosystems (20–23). In tropical rainforests, several species encounter and/or secrete multiple classes of toxins with different target sites, exposing organisms of different lineages to similar yet complex selection pressures, implying the possibility of selection for TSR across many genes and species. For example, the Amazonian snake *Erythrolamprus reginae* and the Chocóan snake *Erythrolamprus epinephelus* coexist with and have been reported to prey on species of several chemically defended amphibian families, including the amine-defended Leptodactylidae, and cardiotonic-steroid (CTS) and TTX-defended Bufonidae (24–31). *Erythrolamprus* snakes also prey on highly toxic frogs of the family Dendrobatidae: the diet of *E. reginae* includes *Ameerega trivittata,* which secretes several alkaloids including histrionicotoxin (HTX) and pumiliotoxin (PTX) (30, 32, 33); *E. epinephelus* is the only known predator of the highly toxic *Phyllobates terribilis* which secretes batrachotoxin (BTX), one of the most potent animal toxins (34). Although closely related, *E. epinephelus* and *E. reginae* are not sister species, and may have evolved the ability to consume toxic amphibians independently. Populations of *E. epinephelus* from Costa Rica exhibit mutations that may allow them to consume TTX-defended prey, possibly frogs of the genus *Atelopus* (11, 12, 35). How *E. reginae* are able to prey on toxic frogs remains unknown. For decades, scientists have focused on the poisonous frogs, paying little attention to the predators involved in their evolution. Yet, the replicated evolution of toxic amphibian consumption makes the genus *Erythrolampus* an ideal system to study microevolutionary processes underlying the evolution of toxin resistance and biased convergent adaptations.

Many neurotoxins present in poisonous frogs interact with voltage-gated sodium channels (VGSCs), a family of proteins that govern the flow of sodium into neurons during an action potential (21, 32, 36). For example, highly toxic alkaloids such as batrachotoxin (BTX) and pumiliotoxin (PTX), and more mildly toxic molecules like histrionicotoxin (HTX) (32, 37), alter action potentials by impairing the function of VGSCs. In non-resistant organisms, exposure to these toxins leads to respiratory and cardiac arrest, pain, and/or death (21, 32). Although VGSCs are targeted by numerous toxins, other proteins involved in neuronal communication can also be targeted (Table S2) (32). Many of the aforementioned toxins are able to bind several members of the VGSC family (21, 32). Therefore, the evolution of TSR should involve adaptation of several VGSC genes.

E. reginae and *E. epinephelus* both consume multiple neurotoxic prey, possibly experiencing strong selective pressures on several different VGSC proteins by potent neurotoxins. Here we explore the degree to which TSR has evolved in VGSCs within and among populations, species, and ecosystems. We expect to identify patterns that match biased convergent evolution that confer TSR, i.e., that they will be shaped by highly similar mechanisms. We anticipate a shared molecular cause of the convergent phenotype because most frog toxins target the same functional regions in the VGSC family, and previous work on these toxins shows a strong pattern of biased convergence in other toxin-resistant organisms. We identify amino acid changes in VGSC orthologs that are likely associated with a TSR phenotype in *E. reginae, E. epinephelus,* and other snakes from the same community, and explore the phylogenetic origin, geographic structure, allelic variability, and linkage of these amino acid changes. Our findings provide an approximation of a resistance mechanism in a predator with a complex toxic diet, and point to complex molecular and/or ecological dynamics as drivers of the coordinated evolution of toxin resistance across multiple genes and species, opening new research avenues to address evolutionary questions in chemically complex biotic interactions.

Results

VGSC Sequence Assembly & TSR Screening

We sequenced 74 genes related to neural communication using target enrichment. We assembled 9 VGSC genes of 8 *Erythrolamprus reginae* individuals and 9 *E. epinephelus* individuals from 3 and 7 different localities, respectively (Fig 1A & Table S2). In addition, we included 21 snake species that coexist in the same habitats but are not known to consume toxic prey, including four additional species of the *Erythrolamprus* genus: five individuals of *E. melanotus*, one of *E. aesculapii*, one of *E. typhlus*, and one individual defined as *E. epinephelus* during the collection but after this study designated as *E.* sp. (Table S1). Although for this study we focus on the 9 genes that make up the VGSC alpha subunit family, we generated additional data on other ion channels that are a rich resource for future research on the molecular mechanisms underlying toxin resistance in snakes (Table S1).

We assembled a complete coding sequence for six of the nine reptilian VGSC genes; for *SCN5A*, *SCN10A*, and *SCN11A*, we were only able to assemble partial sequences, including mostly domain IV (DIV), which has been shown to interact with multiple frog neurotoxins (Fig 2 & Fig S2) (9). To screen for possible sites underlying TSR in these species, we built an amino acid alignment and constructed a phylogenetic and gene family tree with all orthologs and outgroups

(Supp results & Fig S1). Then, instead of focusing on all the substitutions found we narrowed down on the set to positions that fulfilled all of the following three conditions: First, we focused only on specific regions that have been reported to be common toxin-target sites: the voltage-gate in segment 4 (S4), the channel pore (S5 & S6), and p-loops, where the selectivity filter is located (38); Of this set,, we selected positions where identical or similar amino acid substitutions arose in multiple VGSC orthologs; and finally, of these, we selected only the positions where amino acid substitutions were present in more than one *E. reginae* and/or *E. epinephelus* individual but were only present in a maximum of one ortholog in the outgroup species (Fig 1A). Nine homologous positions fulfilled these three conditions (for readability these sites will be referred to as "positions 1–9" or "P1–P9" throughout this study) (Fig 1B). Amino acid substitutions at these nine positions were found in *E. reginae*, *E. epinephelus*, and notably, in a third species, *E.* sp that was previously identified as *E. epinephelus*, but appears to be an evolutionarily independent lineage based on phylogenetic analyses (Fig 2). Four positions were previously reported as part of the TTX binding site (P4, P6, P7, and P8), and mutations at these sites are predicted to provide moderate (P4 & P6) or extreme (P7 & P8) TTX resistance based on computational models or electrophysiology experiments (Fig 1B) (1, 38–40).

Potential TSR substitutions were found in all VGSC genes except for SCN5A. These nine positions were located in the p-loops of domains II (DII), DIII, and DIV, in segment 5 of domain II (DII-S5), and in DI-S6 (Figs 2 & 4). Five of the nine positions are located in DIV, where several TSR mutations have been identified for multiple toxins across animals (e.g. (1, 10, 41, 42)). Seven VGSC orthologs displayed mutations at one or more of the DIV positions (Fig 2). At five of the identified putative TSR positions, the TTX-resistant snake *Thamnophis sirtalis* also has potential TSR substitutions (Fig 2). Using Mixed Effects Model of Evolution (MEME) to analyze the evolutionary rates of VGSC codons, we found that several sites at these positions showed signs of positive selection (in purple, Fig 2). Some additional sites that did not meet the conditions outlined above were also identified by MEME to be under positive selection; these are listed in Dataset S1-Sheet A. Additionally, we found other interesting substitutions located in important functional regions that did not pass the TSR screening conditions. For example, two changes (A445D-*SCN4A* and V1576M-*SCN11A*) each present in only one gene were fixed in the *Erythrolamprus* genus but not shared with other snakes. The A445D-*SCN4A* change also convergently evolved in the poison frogs from the Dendrobatidae family (43). Although we don't focus on these mutations in the present study, they show interesting signatures for future studies. They are reported in Dataset S1-Sheet B.

Geographic segregation and independent origin of TSR sites

Samples from *E. reginae*, *E. epinephelus,* and *E.* sp were collected from three, seven, and one localities, respectively (Fig 3A). To interrogate the geographic segregation and phylogenetic origin of TSR sites relative to the history of *Erythrolampus*, we reconstructed a phylogeny of our focal species using two mitochondrial (*COI*, *16S*) and two nuclear (*c-mos*, *RAG2*) gene sequences. Within the *Erythrolamprus* genus, we found *E. reginae* and *E.* sp to be the sister taxa of the rest of the *Erythrolamprus* samples (Fig 3A & Supp results). However, support for the position of *E.* sp. is low (0.25) and further assessment of the species position in the phylogeny will be necessary. We did not find strong support for genetic structure among the *E. reginae* populations despite the large geographic region we sampled from (Fig 3A & 4A). In contrast, *E. epinephelus* individuals clustered into two groups: group 1 (G1 - triangles) constituted by samples from the inland Chocó rainforests and Cordillera Oriental, and group 2 (G2 - squares) from the Cordillera

Central and Tumaco on the southern Pacific coast of Colombia (Fig 3A). These groupings fall in line with previous work proposing different subspecies, as well as cryptic diversity within *E. epinephelus* (44, 45).

We found high heterogeneity in putative TSR-conferring amino acid changes across individuals and populations of *E. reginae* and *E. epinephelus*. According to ancestral state reconstructions, all of the identified amino acid changes have an independent origin within each of these species (Fig 3B & Table S7), confirming that they evolved convergently rather than in a common ancestor. Most of the putative TSR amino acid changes are not fixed within species, and in some cases even within populations; most commonly, they were found at intermediate frequencies, or at high frequencies but not fixed species-wide (i.e., some heterozygous individuals were found). If we only focus on the amino acid changes that are associated with TTX resistance (P4, P6, P7 & P8), we find that none of them are fixed in *E. reginae*, but three are fixed in *E. epinephelus* (Fig 3B). The TTX-resistant substitutions P7 & P8 - *SCN9A* are shared by all the suborder Serpentes, and have been reported previously (12, 46). Additionally, we did not find any clear correlation between the presence of amino acid changes from P1 to P9 and either geography or population structure, except for the extreme TTX-resistant substitutions in P7 & P8 of the *SCN4A* gene, the muscle-expressed VGSC. Amino acid changes at these two positions in this gene were only found in the Amazonian populations of *E. reginae*, and in all of the G2 *E. epinephelus* individuals. To summarize the extreme variability found in the data, we illustrate the heterogeneity in genotypes at each of the putative TSR positions across the *E. reginae* and *E. epinephelus* samples, including any apparent geographic patterns, in Figs 4 & S2.

Fine-scale variation in and linkage of putative TSR sites

The preceding evidence indicates that TSR evolved under shared molecular mechanisms (biased convergence) in at least some of the nine positions highlighted, as substitutions at the same homologous sites of the VGSC genes appeared independently in three *Erythrolamprus* species. However, there is fine-scale variation in the (potentially) resistant phenotype at the molecular level. For example, if we focus on the sites where amino acid substitutions can provide extreme TTX resistance (P7 & P8), there is variation in the identity of the amino acid change and frequency of homozygosity across orthologs, species, and populations (Fig 5A). In *E. epinephelus*, at least four amino acid combinations were found at P7 and P8 in *SCN1A*: the ancestral “DG” combination, as well as the derived combinations “ND”, “SD”, and the most frequent “SE”. All *E. epinephelus* individuals carried at least one putatively toxin-resistant substitution at these two sites (Fig 5A). Amino acid changes at P7 and P8 in *SCN1A* show a progression in mutational distance from the ancestral genotype “DG”, first to “ND”, which is separated from “DG” by a single mutation at each codon, then to “SD” which adds a second nucleotide substitution to the codon encoding “N”, and finally “SE” which can only be reached through a two nucleotide substitutions per codon (see *SCN1A* gene in Fig 5B).

Of the nine highlighted putative TSR positions, five are found in the DIV p-loop (P5-P9). Thus, we generated haplotype networks for DIV within *E. epinephelus* and *E. reginae* to unveil the genealogical relationships between haplotypes with different amino acid identities at P7 and P8 (Fig 5B). In most cases we found networks consistent with each putative TSR substitution arising once within each species. However, in some instances our results suggest that some variants may have evolved multiple times within a single species. For example, in the *SCN3A* gene in *E. reginae*, the two distant haplotypes carrying the “DV” variant could have originated independently (Fig 5B & samples 2726 and 2335 in Fig. S2), although we note that haplotype networks alone

are not sufficient to recapitulate the origins of a particular mutation, since they don't explicitly account for recombination.

Finally, to explore possible linked segregation between P7 and P8 across orthologs, we calculated pairwise linkage disequilibrium between alleles at these two specific positions. These positions were chosen because there is strong evidence supporting that they confer extreme resistance to TTX (1, 12, 47). We found a relatively strong degree of linkage disequilibrium (LD) between P7 and P8 sites in the *SCN1A*, *SCN4A,* and *SCN8A* orthologs in both species (Fig S3). However, larger population sampling is necessary to make robust conclusions.

Discussion

Putative phenotypic effects of the amino acid changes

This study describes independent origins of putative toxin-resistance-conferring mutations in three species of the *Erythrolamprus* genus: *E. reginae*, *E. epinephelus,* and an undescribed snake, *E.* sp. We show that nine homologous positions across the VGSC family exhibit convergent amino acid changes in regions that are functionally important for neurotoxin resistance (Fig 3B & 4). However, the presence of mutations in the target protein does not necessarily relate to toxin insensitivity, and may be insufficient to explain the resistant phenotype (48, 49). It is thus important to highlight that functional experiments are necessary to confirm whether specific substitutions provide any TSR for biologically relevant toxins. With that caveat in mind, given the patterns of selection and convergent evolution in our data, what is known about TTX resistance, and the notion that VGSC genes tend to be under strong purifying selection (50, 51), we hypothesize that it is likely that substitutions at the positions we identify affect *E. reginae* and *E. epinephelus* neurotoxin resistance phenotypes.

From the nine putative TSR positions highlighted in this study, several amino acid changes at four of these positions (P4, P6, P7, and P8) can provide TTX resistance, and substitutions at the other five positions are shared with several other neurotoxin-resistant organisms (Fig 4). Several electrophysiology experiments and computational models in different organisms provide evidence that TTX resistance is conferred by substitutions at P4, P6, P7 & P8 (1, 12, 41, 47, 52). For P4, in computational models showed that replacing the wild-type aspartic acid in P4 of the rat SCN2A with polar-charged amino acids provided moderate TTX and STX resistance (41, 52). For P6, electrophysiology experiments showed that amino acid changes cause moderate TTX resistance in *T. sirtalis* snakes and *Taricha* newts (1, 13, 47). For P7 and P8, electrophysiology experiments have shown that amino acid changes found in the *T. sirtalis SCN4A* channel causes extreme TTX resistance (12, 46). The same asparagine that confers TTX resistance in *T. sirtalis* is present in the *SCN1A, SCN2A, SCN3A* and *SCN4A* proteins of *E. reginae*, *E. epinephelus*, and *E.* sp. (Fig 2 & see protein names in Table S2). In addition, we confirmed that all the snake species in this study, including all sampled *Erythrolamprus* individuals, share the extreme TTX resistant changes at P7 & P8 - *SCN9A* and at P8 - *SCN11A* that were hypothesized to be ancestral to snakes, as well as changes in P6 that were are reported in the *SCN8A* and *SCN11A* channels in some other species of the Colubridae family (Fig 2 & Fig S2) (12, 46). However, because we could not retrieve the DI, DII, and DIII from *SCN5A*, *SCN10A*, and *SCN11A*, we could not verify whether individuals possessed additional TTX-resistant changes that have been hypothesized to be ancestral to snakes reported by (46). Concordant with electrophysiological evidence, multiple TTX-resistant organisms exhibit changes at these positions (Table S6) (see references in (9)). Based on the points above, the assumption that at least some of the identified mutations in *E.*

reginae, *E. epinephelus* and *E.* sp. are likely to be involved in TTX resistance seems reasonable (Fig 4). Although the phylogenetic position of *E.* sp. is uncertain, *E.* sp. possess different amino substitutions than the other two species (*E. reginae* and *E. epinephelus*) at some putative TSR positions, providing evidence for a possible third independent origin of toxin-resistance (Fig 2).

The previously discussed positions have been reported to cause a TTX-resistant phenotype. On the other hand, changes in P1, P2, P3, P5, and P9 are shared with different toxin-resistant vertebrates, but there is no available experimental data regarding their effect on toxin resistance (Fig 2). Thus, it is important to note that some of these mutations may arise from mechanisms unrelated to toxin resistance. However, we hypothesize that some of these positions have a moderate or compensatory contribution to toxin resistance because the substitution is not directly located within the inner pore or selectivity filter of the channel (Fig 2). For example, amino acid changes in P1 and P9 are both shared with the *SCN4A* from dendrobatid frogs, but are not located directly in the DIV p-loop (Fig 2, Table S6). Changes at P2, the only position located in the DII-S5 of the *SCN4A* channel pore, identified in *E. reginae* and *E. aesculapii,* are shared with the TTX-resistant snakes from the *Thamnophis* genus and the hog-nosed snake *Heterodon platirhinos*, which preys on the TTX-bearing newt *Notophthalmus viridescens* (Table S6) (49, 53). Although found in predators of tetrodotoxic newts, the P5 location does not correspond to any TTX-binding site and has not been highlighted before in any toxin-resistant organism (38, 54).

The convergent evolution of the VGSCs between species and paralogs

The presence of convergent or similar amino acid substitutions at the same homologous sites across genes in at least three species of the *Erythrolamprus* genus reveals that toxin resistance in Royal Ground snakes has likely evolved – at least partly – using a shared molecular mechanism that could be described as biased convergent evolution (16). Eight of nine VGSC genes contained mutations that encode amino acid changes at the putative TSR positions. These changes vary substantially across genes in the VGSC family (Fig 2). Although we do not possess information about the tissue-specific expression of these channels in *Erythrolamprus* snakes, the VGSC gene family in snakes contains nine genes that play different roles in the central and peripheral nervous system. In mammals, *SCN1A*, *SCN2A* and *SCN3A* are expressed in the brain, *SCN4A* is expressed in the skeletal muscle, *SCN5A* in the cardiac muscle, *SCN8A* and *SCN9A* in the peripheral nervous system (the *Anolis carolinensis* lizard exhibits the same expression pattern, Fig S4) (55), and in *T. sirtalis*, *SCN10* and *SCN11A* in small sensory neurons (46).

The presence of heterogeneous amino acid changes in several VGSC orthologs within and among species makes clear that further research is necessary to understand how toxin sensitivity varies across tissues in *E. reginae*, *E. epinephelus*, and *E*. sp and among different toxic molecules. For example, it has been previously reported that extreme TTX resistance in *SCN5A* is shared across all tetrapods, that extreme TTX resistance in *SCN9A* is shared across snakes, and that differential TTX sensitivity is present in the remaining VGSCs (12, 46, 56). However, to our knowledge, we report the first potential evidence of TTX-resistance-conferring substitutions in the brain-expressed *SCN1A, SCN2A*, and *SCN3A* VGSC orthologs in reptiles. Interestingly, amino acid changes at the TTX-binding sites P4 and P5 are only present in brain-expressed genes. As highlighted, amino acid changes at P4 can provide moderate resistance to TTX and STX (41, 52). Amino acid changes at P5 have not been experimentally tested against toxins. However, P5 is one amino acid distanced from a position where specific substitutions provide

moderate TTX resistance in rat sodium channels, and where tetrodotoxic newts exhibit mutations in the *SCN1A* and *SCN3A* genes (Fig 2) (47). In *Anolis carolinensis* they are expressed exclusively in the brain, which suggests that *E. reginae* and *E. epinephelus* exhibit TTX resistance in brain tissues (Fig S4) (57). Why might this be? TTX may move across the blood-brain barrier in snakes, as occurs in pufferfish (58). Alternatively, these substitutions may be involved in resistance to other toxins that do cross the blood-brain barrier. Finally, these proteins may be expressed in tissues other than the brain, such as the adrenal glands (Fig S4).

In this study, we propose that a pattern of linkage disequilibrium, caused by selection and not necessarily by physical linkage among some positions, is the mechanism that maintains this coordinated evolution across tissues. The variation in substitutions among individuals and proteins suggest multiple or intermediate fitness peaks present across tissues. For example, we show a correlation between positions P7 & P8 in *SCN1A*, *SCN4A* and *SCN8A* separately in *E. reginae* and *E. epinephelus* samples (Fig S3). In *T. sirtalis* snakes, these genes are located on different chromosomes (59) suggesting an independent origin of the mutations and a pattern of linkage caused by selection. However, some genes of the VGSC family are located on the same chromosome, suggesting that physical linkage and/or gene conversion could also contribute to the appearance of this pattern (13, 59). This evidence of linked segregation between genes expressed in different tissues suggest that the presence of differential TSRs between VGSC genes is necessary for the resistant phenotype.

Ecological context and relevance for VGSC evolution in *Erythrolamprus* snakes

Our study has shown that resistance to TTX is highly plausible for *E. reginae*, *E. epinephelus,* and *E.* sp (Fig 3B). Thus there are multiple ecological implications of the TTX-resistant phenotype according to the distribution and diet of each of these species. The endangered genus *Atelopus* and the frog *Colostethus panamansis* are the only reported amphibians with TTX in these species' ranges (35, 60, 61). In Costa Rican populations of *E. epinephelus*, substitutions at P6, P7, and P8 in *SCN4A, SCN8A, SCN10A, SCN11A* have been previously reported, indicating a broad geographic distribution of resistance alleles that could match with the presence of *Atelopus* frogs (11, 12, 46). These frogs have suffered a recent and drastic population decline, but in the past, they were abundant and sympatric with *Erythrolamprus* snakes across multiple biomes (62, 63). In the *Colostethus* genus, the phylogenetic distribution of TTX secretion is still unclear. Although proposed for *C. ucumari* from visual observations, the presence of TTX was never confirmed in this species, and recent studies have not found evidence of TTX in *C. imbricolus* or in the skin microbiome of *C. panamansis* frogs (20, 64, 65). Furthermore, there are no known *Colostethus* species distributed in sympatry with *E. reginae*.

Additional conditions could explain the evolution of TTX-resistant substitutions. First, these snakes could prey on uncharacterized TTX-defended amphibians, or other tetrodotoxic animals. Observations in the field suggest that insects are consumed by *E. reginae* juveniles (pers. obvs. Dario Alarcón Naforo), although in the literature there are no tetrodotoxic insects reported from the Colombian regions. The Geoplanidae subfamily of flatworms, common in the Amazonian rainforest, contains terrestrial tetrodotoxic species. Although not reported in these snakes' diet (66), several snake generalists can exhibit an ontogenetically and ecologically differential diets, which can include insects, worms, and slugs (eg. (67, 68)). Our understanding of TTX presence in the tropics is limited, and further research is necessary to trace the presence of this molecule in the Andes, Amazon, and Chocó rainforests. Alternatively, the TTX-resistant substitutions

exhibited by *Erythrolamprus* snakes could provide resistance to additional toxins. Two toxic molecules have been reported to bind at the same sites as TTX: STX and μ-conotoxin (38, 69–71). These two toxins are found in freshwater organisms that could be part of the snake diet. However, there is a lack of surveys to trace the possible presence of STX and μ-conotoxin in terrestrial organisms. While derivatives of TTX, STX, and μ-conotoxin could exhibit similar effects, in our knowledge there are no other toxins known to be secreted by frogs that compete with TTX. Nevertheless, some of the substitutions found in this study could provide resistance against other frog toxins. For example, PTX-B found in frogs from the *Oophaga* genus competes against *Scorpio* toxins and brevetoxins that bind to DI-S6 and DIV S3-S4 (32, 38, 72, 73), and HTX found in *Ameerega* and other dendrobatid frogs inhibits the binding of [3H]BTX-B that affects the S6 channel pore (32, 39, 74). In addition, amino acid changes in the DIII p-loop provide BTX resistance (39). Some putative TSR positions identified in this study and shared by *E. reginae* and *E. epinephelus* are located in these protein regions (Fig 2). Based on limited diet observations, the toxins in *Ameerega* frogs and the toxins found in *Phyllobates* and *Atelopus* frogs may be drivers of VGSC evolution in *E. epinephelus* and *E. reginae*, respectively (11, 33, 34). However, further physiological assays and ecological information are necessary to test these hypotheses. Finally, while we think it unlikely, it is plausible that these positions are not involved in toxin resistance at all; instead, they may be related to other physiological function and variation in these snake species.

Evolutionary genetics of TSR allele polymorphisms

TSR is a convergent molecular mechanism of toxin resistance that is shared but not identical in multiple species of *Erythrolamprus* snakes. At a finer molecular level, we found that the identity and presence of different amino acid changes at P1–P9 are highly variable, suggesting that the protein function and resistance varies across tissues and populations. There are at least four levels of molecular variation in this study that would contribute to organismal-level function and resistance. A first level of variation is the different amino acid changes segregating at the same position (e.g. Fig 5A). These amino acid changes could differentially impact the protein function, producing multiple fitness peaks or exhibiting intermediate variants in the mutational path between the non-resistant variant and resistant variant (see *SCN1A* and *SCN4A* in Fig 5B). Alternatively, these different amino acid changes in the same position could produce the same toxin-resistant phenotype (14, 75). A second level of variation is the presence and absence of substitutions across the P1–P9 positions. In our data, some samples exhibit the complete array of putative TSR changes, while others have an “incomplete” version, even within a specific population (Fig 3B and Fig 5A). This pattern could emerge from balancing selection, as well as from incomplete orand soft selective sweeps, but distinguishing between these evolutionary mechanisms remains a challenge and requires genome-wide data (76, 77). A third level of variation is the presence and absence of amino acid changes with a potentially compensatory function. In this study, we defined compensatory amino acid changes as non-synonymous substitutions that evolved to maintain the protein function despite the adverse effects of TSR substitutions. We suggest that some of the putative TSR positions have a compensatory effect, for example, if the substitution is not directly located close to a toxin binding site (eg: P3 and P9 in Fig 2) (e.g. (75)). Finally, a fourth level of variation is the differential presence of amino acid substitutions at TSR positions across the VGSC family that has been discussed previously.

The extensive molecular variation present at P1–P9 across the VGSC family is consistent with a selection regime that favors polymorphism. Balancing selection, soft selective sweeps and local adaptation could both produce some of the patterns that we encounter in our data. These mechanisms have been previously reported in predator-prey coevolutionary relationships, including in snake predators (78, 79). Although more extensive population sampling and genome-wide population data would allow us to discriminate between selection regimes in the future, we suggest that two interacting processes help maintain these polymorphisms across and within populations.

First, balancing selection and soft selective sweeps: it is possible that TSR substitutions impair sodium channel function, resulting in a trade-off between the toxin resistance adaptation and organism-level performance (19, 49, 80). Amino acid substitutions in *T. sirtalis* snakes at positions P6, P7, and P8 alter the conductance of the muscular VGSCs, causing reductions in muscle performance and snake speed (19, 80). The ecological relevance of this reduction of function in the snakes' habitat has not been tested yet. However, we hypothesize that the impact of the trade-off between toxin resistance and protein function on fitness depends on the molecular and ecological background, which can vary over time and space. We provide evidence for allelic polymorphism at multiple TSR positions in the best sampled population (*E. reginae* from the Amazon), which, together with high levels of linkage disequilibrium between haplotypes at P7 and P8 in genes located in different chromosomes in the *T. sirtalis* genome (Fig S3), may point to balancing selection and other mechanisms at the genetic or population level that maintain variation (Figs 5A & S2). Such a dynamic would maintain intermediate allele frequencies through heterozygous advantage and/or fluctuating selection dependent on, for instance, the abundance of specific chemically defended prey. Eventually, the evolution of compensatory mechanisms, which may be encoded by additional variants, could decrease the cost of TSR genotypes and lead to their fixation. It is possible that some of the allelic diversity observed is due to intermediate alleles in the mutational path between susceptible and resistant variants that are still segregating but will eventually go extinct due to the intermediate phenotypes they produce.

Second, local adaptation: the large geographic and ecological range of these species could promote local adaptation, with gene flow between locally adapted populations resulting in within-population polymorphisms. Local adaptation is a common mechanism for the evolution of VGSCs in the TTX-resistant *Thamnophis sirtalis* snakes (1, 18) and may explain the diversity of VGSC alleles observed in this study (Fig 5). We propose that geographic heterogeneity of selection pressures contributes to and promotes a dynamic evolution of VGSCs. Prey availability, the specific toxic molecules, and the level of toxicity that these snakes encounter are likely to be highly variable in space. In general, we do not find a clear or unique geographical pattern that explains the presence of particular polymorphisms (Figs 3A & 5A). The Chocó and Amazon harbor a wider diversity of poison frogs than other biogeographic regions of Colombia where *E. reginae* and *E. epinephelus* occur (81). Thus, we hypothesized that *E. epinephelus* populations located in the Chocó rainforest and *E. reginae* populations situated in the Amazon rainforest would exhibit more TSR-related substitutions, if substitutions contribute in an additive manner to toxin resistance. Although we did not find a greater number of substitutions in these populations, we found that the TSR mutations in the muscle-expressed *SCN4A* channel were only present in individuals of the *E. reginae* Amazon population and in higher frequency present in *E. epinephelus* monophyletic group 1, which were collected in the Chocó rainforest and the Western cordillera (Figs 3A & 5A). The evolution of resistant variants in the *SCN4A* channel is common in vertebrate predators and prey exposed to high levels of neurotoxins, such as TTX, that target

VGSCs (1, 10, 11, 82). Thus, this is consistent with a stronger selective pressure in the Amazonian and Chocó rainforest populations to evolve toxin resistance. However, it seems that in *E. epinephelus* these substitutions are present in populations with lower poison frog diversity such as the Western cordillera (sample 2743). Finally, we found that between the two species, the number of putative TSR substitutions is greater in *E. epinephelus* than in *E. reginae* (Fig 2). We suggest that *E. epinephelus* is under stronger selective pressure or that maintaining these substitutions is physiologically less costly than in *E. reginae*, a fact that could be explained by the higher number of highly toxic dendrobatid and bufonid frogs documented in the Chocó rainforest in comparison with the Amazon (81). Nevertheless, broader geographic and within-population sampling, functional data on the physiological effects of the observed mutations, and further information on the distribution and toxicity of amphibian chemical defenses (e.g. (35)) are essential to understand the population dynamics of the resistant phenotype in these two species. Overall, we suggest that the molecular diversity found in VGSCs in *E. reginae* and *E. epinephelus* is maintained by balancing selection as well as local adaptation and gene flow that causes multiple fitness peaks within and/or and between populations.

Concluding Remarks

In conclusion, this work introduces a new model system for studying eco-evolutionary adaptations of toxin resistance in the highly chemically and biologically diverse forests of South America. This model provides an opportunity to investigate coordinated evolution across gene families in relation to toxin resistance, as well as convergent evolution between species. Although we focus on the VGSCs, we provide extended sequencing data of other ion channels for future research on the molecular mechanism of toxin resistance. Urgent research on these topics is fundamental to understanding the impact of declining species and the resulting loss of complexity in the chemical composition of the forests and the maintenance of biodiversity.

Materials and Methods

Sample collection and target enrichment sequencing

We collected tissue samples from 40 snakes from different locations across Colombia, spanning multiple ecosystems including plain grasslands, and lowland and montane wet forests, under permit 1177 (October 9, 2014, file No. IDB0359), granted by the Colombian Authority for Environmental Licenses (ANLA; Table S1). Collection protocols were approved by the Universidad de los Andes Bioethics Committee (protocol number C.FUA 14-018M). For each sample, we obtained mouth swabs, muscle tissue, or liver tissue, subsequently stored in 70% ethanol or RNAlater® (Life Technologies, Carlsbad, CA) at –80 °C. We also obtained tissue samples (tail, muscle, or liver) through loans from the Instituto de Ciencias Naturales (ICN) at the Universidad Nacional de Colombia (Table S1). Our final dataset consisted of 9 *E. epinephelus* individuals corresponding to 7 different localities (Fig 3A), 8 *E. reginae* individuals corresponding to 3 localities, and 4 *E. melanotus* individuals corresponding to 3 localities, one Amazonian sample of *E. typhlus*, one Amazonian sample of *E. aesculapii*, as well as 17 individuals from 12 genera which were used as outgroups (Table S1).

We used target enrichment and Illumina sequencing to obtain around 200 Kb that corresponded to the complete sequence of 74 genes from 14 gene families involved in neurological functions, and therefore putatively involved in neurotoxin resistance, and two nuclear genes commonly used in phylogenetic reconstruction (Table S2). For this study we focus on the 9 genes that make up the voltage-gated sodium channel alpha subunit family (VGSC family). All generated data are publicly available on NCBI with BioProject ID PRJNA1055115. We extracted DNA using the Qiagen DNeasy kit and quantified it using a Qubit dsDNA HD Assay Kit (Thermo Fisher Scientific). We reconcentrated some samples using a SpeedVac (Thermo Fisher Scientific) until they reached a minimum DNA concentration threshold of 40 ng/ul. We fragmented DNA to obtain 400-bp fragments by running three cycles of 30 seconds using a Brandon 2800 ultrasonicator, and prepared 40 genomic DNA libraries using the Accel-NGS 1S Plus Swift bioscience™ library preparation kit for the Illumina platform, following the recommendations of the manufacturer, except for the purification step when we used the AMPure XP beads (Beckman Coulter) for an average size selection of 400 bp. We indexed each sample using dual identifiers (Dual-indexing barcodes) from the Swift bioscience™ 1S Plus Dual Indexing kit. For a final quality check, we used Agilent High Sensitivity DNA® kit and the Qubit dsDNA HD Assay kit. On average we obtained libraries with 400-bp fragment sizes at 4 nM. Library preparations were performed at the Universidad de los Andes in Bogotá, Colombia.

We enriched the target genes using a custom set of MYbaits® in-solution (MYcroarray) enrichment probes, designed by the company using gene annotations extracted from the *Python bivittatus* (Genbank accession number: AEQU02000001.1) and *Ophiophagus hanna* genomes (PRJNA201683), or gene sequences from *Thamnophis sirtalis, Erythrolamprus reginae* and *Protobothrops mucrosquamatus* generated in previous studies (Table S2). We chose the most relaxed design of the probes (Relaxed-4) to account for the wide phylogenetic breadth of our samples. We pooled 2 to 3 libraries for each capture, depending on the DNA concentration, to perform 16 enrichment reactions using the provider's protocol, and we purified the enriched libraries using Dynabeads® MyOne™ Streptavidin C1 (Life Technologies). Finally, we sequenced all libraries using one lane of the Illumina NextSeq500 platform (150-bp paired-end reads) at ACGT, Inc, Wheeling, IL. The mean number of reads obtained was 1.5 M (SD = 668 K) per sample (Table S1).

VGSC family sequence annotation and TSR screening

Read quality was evaluated using FastQC v0.10.1 (83). We removed adapters and quality-trimmed reads using Trimmomatic v0.32 (84). To generate nucleotide sequences for the VGSC family we used Bowtie2 v2.3.4.1 to map the cleaned reads against the *Pantherophis guttatus* genome (Genbank ID: GCA_029531705.1). We generated phased consensus sequences using Picard v2.9.0 (85) and samtools v1.18 (86). We used bcftools v1.12 (86) to call genotypes. The coordinates for each gene in the *P. guttatus* genome were annotated manually using Hmmer v3.1b2 (87) against the bait sequences (Table S2), and sequences were extracted using bedtools/2.28.0 (88). Finally, we used blast v2.7.1+ (89) to annotate the exons against our sequences, and extracted and concatenated them to assemble the coding sequences for each gene (Dataset S3). The exons used as query in blast were *SCN1A, SCN2A, SCN3A, SCN4A, SCN8A* and *SCN9A* from *T. sirtalis* exons, previously annotated by (90). For the *SCN10A* and *SCN11A* genes, we used *P. guttatus* exon annotations, and for *SCN5A*, we used *Xenopus tropicalis* and *Gallus gallus* exons. Only the domain IV (DIV) of the latter three genes was

recovered. Table S3 contains the annotated coordinates for each gene on the *P. guttatus* genome and GenBank ID of the query exon sequences.

The high conservation among VGSC orthologs poses challenges for gene annotation and increases the probability of assembling chimeric sequences. Thus, we generated a gene family tree using the consensus sequences and outgroups to verify the gene identity of each sequence (Fig S1, Table S4 & Dataset S2). We translated and aligned the sequences using Clustal Omega v1.2.3 as implemented in Geneious v2021.2.2 (https://www.geneious.com). Then, using the CIPRES gateway (91), we estimated a maximum likelihood VGSC protein family tree in IQtree v2.1.2 (92) under the LG model, and assessed support with ultrafast bootstraps using default parameters. We visualized the resulting tree in iTol v5 (93). The interactive tree can be displayed using the following link or ID (https://itol.embl.de/export/20111332514600816890249 34 or ID 20111332514600816890249 34). Our reconstruction showed monophyletic groupings by orthologous gene, confirming our annotations and showing no evidence of chimeric sequences.

The lack of clear information regarding the diet of the *Erythrolamprus* snakes did not allow us to make comparisons among specific molecules that these snakes might encounter regularly or rarely. However, at least a few toxins that are found in the reported prey and in sympatric poisonous frogs target the VGSC family (eg: TTX, HTX, BTX, PTX, etc) (32). The target sites of TTX and BTX have been characterized using x-ray crystallography (21, 37, 69, 94), but less is known about binding sites or activities of the other toxins (21, 37). Thus, to screen for substitutions potentially related to toxin insensitivity, we focused on sites previously linked to TTX resistance in *T. sirtalis*, as well as those that fulfilled the three requirements shown in Fig 1. Changes present in a single haplotype of *E. reginae* or *E. epinephelus* were not included in our analyses, but are listed in Database S1. To determine the ancestral state of the amino acid changes we reconstructed ancestral sequences for each protein using Hyphy (95). This program calculates a joint maximum likelihood according to a previous fitted model FitMG94. Functional regions were annotated based on (5). Sequence residues are numbered based on *Mus musculus* protein sequences (See Uniprot number at Table S4).

Phylogenetic tree reconstruction

To interpret the reconstructed amino acid substitutions in the context of *Erythrolamprus* genus phylogenetic history, we used *c-mos* and *RAG2* sequences (from target sequencing Table S2) and two mitochondrial loci obtained through PCR and sanger sequencing to reconstruct a phylogenetic tree for our samples. We amplified the *CO1* gene using primers dgLCO-1490 (5'-GGT CAA CAA ATC ATA AAG AYA TYG G-3') and dgHCO-2198 (5'-TAA ACT TCA GGG TGA CCA AAR AAY C-3') (96), and the *16S* gene using 16Sbr-H (5'-CCGGT CTGAA CTCAG ATCAC GT-3') and 16Sar-L (5'- CGCCT GTTTA TCAAA AACAT-3') (97), following the PCR conditions described in the respective papers. After aligning each set of sequences with MAFFT using the *mafft-linsi* option (98), we estimated maximum likelihood trees separately for each gene using IQ-TREE v2.1.2 (92), and assessed support using ultrafast bootstrapping with the default parameters in CIPRES gateway (91). We then concatenated the two mitochondrial genes and reran the analysis. Finally, we built a species tree using ASTRAL and estimated the multilocus 2-stage bootstrap values developed in this program (Figs 3A & 5A)(99, 100).

Positive selection tests

We screened VGSC sequences for signatures of positive, diversifying selection in a phylogenetic context using the Mixed Effects Model of Evolution, MEME, implemented in HyPhy, using default parameters (101). MEME is a branch-site model that employs maximum likelihood to test for positive selection at each site, not assuming a ω single value across the tree (101). We conducted a codon-based selection test for the VGSC family genes from an alignment of exclusively the *Erythrolamprus* genus samples (Dataset S3). This test was run on the DataMonkey server using default parameters (102) and the results were visualized on Hyphy Vision (103).

Intraspecific variation in VGSC genotypes

Our data revealed that several mutations putatively involved in TSR were not fixed within *Erythrolamprus* species. Therefore, to further explore patterns of intraspecific variation we built minimum-spanning haplotype networks (epsilon = 0) in PopArt (104) for the DIV of the VGSC genes (Fig 5B), where the majority of putative TSR mutations were found. In addition, we calculated nucleotide diversity (π), number of segregating sites, number of parsimony-informative sites, and Tajima's D, testing for $D \neq 0$ with a permutation-based p-value using PopArt (Table S5). Networks and statistics were calculated independently for *E. reginae* and *E. epinephelus* populations, as well as for the *E. melanotus* samples, which did not exhibit the potential TSR but was used as a 'control' group for comparison. Finally, we show the co-segregation of SNPs related to toxin resistance by calculating the square correlation (r^2) of a biallelic polymorphism at the domain IV of the VGSC. To obtain a pairwise statistic we used the *LDscan* function from the *pegas* R package (105). The results were plotted using ggplot2 and plotly packages in Rstudio (106, 107) (Fig S3).

Data availability

All sequence data are publicly available on NCBI with BioProject ID PRJNA1055115.

Code availability

All pipelines used are publicly available on https://github.com/esperando370

List of abbreviations

VGSC = Voltage-Gated Sodium Channel
TSR = Target-Site Resistance
D = Domain of the protein
S = Segment of the protein
TTX = Tetrodotoxin
BTX = Batrachotoxin
HTX = Histrionicotoxin
PTX = Pumiliotoxin
STX = Saxitoxin
CTS = Cardiotonic steroids
LRT = Likelihood Ratio Test

P = Position
LD = Linkage disequilibrium

Acknowledgments

We thank the Program for Basic Science of Colciencias 712-2015 (No. 120471249694) and the seed projects at the Universidad de Los Andes for funding this study. We also thank the Russell E. Train Education for Nature Program (EF14103) from the World Wildlife Fund (WWF) and the National Institutes of Health (NIH NIGMS #R35GM150574) that funded VRC expenses during the writing process. RM was partially supported by the Michigan Society of Fellows. Thanks to the Instituto de Ciencias Naturales at the Universidad Nacional, Fernando Vargas Salinas at the Universidad del Quindío, Jhon Tailor Rengifo at the Universidad Tecnológica del Chocó, Jhonatan David Echavarria, Nicomedes Asprilla and Elkin de Jesús Asprilla for loaning samples for this study. Thanks to Reserva Natural Taninboca in Leticia and the Reserves in Bajo Calima, Valle del Cauca and Puerto Salgar, Cundinamarca for granting permission to work there. We are very grateful for all the local guides and workers that helped us and kindly shared time and knowledge with us. Also, for having the opportunity to observe and interact with snakes and frogs, observe them closely and share a home with them, the forest, and cities where they live. Special thanks to the great friends we made during the Master of Biological Sciences at the Universidad de Los Andes: Camilo Rodríguez, Pablo Palacios, Diana Motta, Iván Beltrán, Mabel González, Mileydi Betancourth-Cundar, Leonardo Moreno, Jorge Díaz Riaño, Leidy Barragán, Catalina Ramírez-Portilla, among others. They taught VRC how to work in the field, analyze data, understand science and most importantly make those years, very happy years. Finally, we acknowledge that our fieldwork was conducted in territories where local communities continue to face exclusion from scientific endeavors and suffer from the imposition of capitalist and colonial activities. Historically, science has contributed to these activities, and regrettably, there is no assurance that the findings from this or other biological research will not perpetuate these power structures in the future. Nevertheless, we affirm our commitment to conducting scientific work that actively opposes the imposition of patriarchy, capitalism and colonialism on any body or territory. We hope that any use or application derived from this work will not be used to further these purposes. The Spanish translation was made using DeepL.com and then edited by VRC (Available Dryad).

References

1. S. L. Geffeney, E. Fujimoto, E. D. Brodie, E. D. Brodie, P. C. Ruben, Evolutionary diversification of TTX-resistant sodium channels in a predator-prey interaction. *Nature* **434**, 759–763 (2005).
2. L. Després, J.-P. David, C. Gallet, The evolutionary ecology of insect resistance to plant chemicals. *Trends Ecol. Evol.* **22**, 298–307 (2007).
3. R. D. Tarvin, *et al.*, Interacting amino acid replacements allow poison frogs to evolve epibatidine resistance. *Science* **357**, 1261–1266 (2017).
4. S. N. Caty, *et al.*, Molecular physiology of chemical defenses in a poison frog. *J. Exp. Biol.* **222** (2019).
5. F. Abderemane-Ali, *et al.*, Evidence that toxin resistance in poison birds and frogs is not rooted in sodium channel mutations and may rely on “toxin sponge” proteins. *J. Gen. Physiol.* **153** (2021).
6. A. Alvarez-Buylla, C. Y. Payne, C. Vidoudez, S. A. Trauger, L. A. O’Connell, Molecular physiology of pumiliotoxin sequestration in a poison frog. *PLOS ONE* **17**, e0264540 (2022).
7. Z. Chen, *et al.*, Definition of a saxitoxin (STX) binding code enables discovery and

characterization of the Anuran saxiphilin family. [Preprint] (2022). Available at: https://www.biorxiv.org/content/10.1101/2022.06.09.495489v1 [Accessed 20 July 2022].
8. R. D. Tarvin, K. C. Pearson, T. E. Douglas, V. Ramírez-Castañeda, M. J. Navarrete, The Diverse Mechanisms that Animals Use to Resist Toxins. *Annu. Rev. Ecol. Evol. Syst.* **54**, null (2023).
9. J. van Thiel, *et al.*, Convergent evolution of toxin resistance in animals. *Biol. Rev.* **97**, 1823–1843 (2022).
10. M. C. Jost, *et al.*, Toxin-resistant sodium channels: Parallel adaptive evolution across a complete gene family. *Mol. Biol. Evol.* **25**, 1016–1024 (2008).
11. C. R. Feldman, E. D. Brodie, E. D. Brodie, M. E. Pfrender, Constraint shapes convergence in tetrodotoxinresistant sodium channels of snakes. *Proc. Natl. Acad. Sci. U. S. A.* **109**, 4556–4561 (2012).
12. J. W. McGlothlin, *et al.*, Historical Contingency in a Multigene Family Facilitates Adaptive Evolution of Toxin Resistance. *Curr. Biol.* **26**, 1616–1621 (2016).
13. K. L. Gendreau, A. D. Hornsby, M. T. J. Hague, J. W. McGlothlin, Gene Conversion Facilitates the Adaptive Evolution of Self-Resistance in Highly Toxic Newts. *Mol. Biol. Evol.* **38**, 4077–4094 (2021).
14. M. Karageorgi, *et al.*, Genome editing retraces the evolution of toxin resistance in the monarch butterfly. *Nature* **574**, 409–412 (2019).
15. S. Mohammadi, *et al.*, Concerted evolution reveals co-adapted amino acid substitutions in Na+K+-ATPase of frogs that prey on toxic toads. *Curr. Biol.* (2021). https://doi.org/10.1016/j.cub.2021.03.089.
16. A. A. Agrawal, Toward a Predictive Framework for Convergent Evolution: Integrating Natural History, Genetic Mechanisms, and Consequences for the Diversity of Life. *Am. Nat.* **190**, S1–S12 (2017).
17. C. Natarajan, *et al.*, Predictable convergence in hemoglobin function has unpredictable molecular underpinnings. *Science* **354**, 336–339 (2016).
18. C. R. Feldman, E. D. Brodie, E. D. Brodie, M. E. Pfrender, The evolutionary origins of beneficial alleles during the repeated adaptation of garter snakes to deadly prey. *Proc. Natl. Acad. Sci. U. S. A.* **106**, 13415–13420 (2009).
19. M. T. J. Hague, *et al.*, Large-effect mutations generate trade-off between predatory and locomotor ability during arms race coevolution with deadly prey. *Evol. Lett.* **2**, 406–416 (2018).
20. M. C. González Montoya, Eco-metabolomics approach for understanding the chemodiversity of cocktails found on poison frogs. (2021).
21. J. W. Daly, H. Martin Garraffo, T. F. Spande, “Alkaloids from Amphibian Skins” in *Alkaloids: Chemical and Biological Perspectives*, (Elsevier, 1999), pp. 1–161.
22. G. P. Asner, *et al.*, Amazonian functional diversity from forest canopy chemical assembly. *Proc. Natl. Acad. Sci.* **111**, 5604–5609 (2014).
23. D. Salazar, *et al.*, Origin and maintenance of chemical diversity in a species-rich tropical tree lineage. *Nat. Ecol. Evol.* **2**, 983–990 (2018).
24. A. Jiménez-Ortega, J. Renjifo, Y. Garcia, Una aproximación a la herpetofauna (anfibios y reptiles) del municipio de Novita departamento del Chocó – Colombia. 39–44 (2004).
25. J. D. Lynch, Discovery of the richest frog fauna in the world-an exploration of the forests to the north of Leticia. *Rev. Acad. Colomb. Cienc. Exactas Físicas Nat.* **29**, 581–588 (2005).
26. M. A. Pinto-Erazo, M. L. Calderón Espinosa, G. F. Medina Rangel, M. Á. Méndez Galeano, Herpetofauna de dos municipios del suroeste de Colombia. *Biota Colomb.* **21**, 41–57 (2020).
27. A. O. Gallardo, E. Carrillo-Chica, J. E. V. Lorenzo, ANFIBIOS Y REPTILES del Aeropuerto Alfredo Vásquez Cobo. (2022).
28. Instituto Humbolt, Herpetofauna de ocho Biodiverciudades de Colombia - Bioblitz 2022. (2022). Available at: http://i2d.humboldt.org.co/resource?r=herp_bioblitz_2023 [Accessed 6 May 2023].
29. J. T. R. Mosquera, M. Y. R. Palacios, L. M. R. Albornoz, Colección Científica de

Referencia Zoológica del Chocó- Herpetología. (2022). https://doi.org/10.15472/sz41lm.
30. L. P. P. Albarelli, M. C. Santos-Costa, Feeding ecology of Liophis reginae semilineatus (Serpentes: Colubridae: Xenodontinae) in eastern Amazon, Brazil. *Zool. Curitiba* **27**, 87–91 (2010).
31. E. J. Michaud, J. R. Dixon, Prey items of 20 species of the Neotropical colubrid snake genus Liophis. *Herpetol. Rev.* **20**, 39–41 (1989).
32. J. C. Santos, R. D. Tarvin, L. A. O'Connell, A Review of Chemical Defense in Poison Frogs (Dendrobatidae): Ecology, Pharmacokinetics, and Autoresistance in *Chemical Signals in Vertebrates 13*, B. A. Schulte, T. E. Goodwin, M. H. Ferkin, Eds. (Springer International Publishing, 2016), pp. 305–337.
33. A. Pašukonis, M.-C. Loretto, "Predation on the Three-striped poison frog, Ameerega trivitatta (Boulenger 1884; Anura: Dendrobatidae), by Erythrolamprus reginae (Linnaeus 1758; Squamata: Collubridae)" (2020).
34. C. W. Myers, J. W. Daly, B. Malkin, A dangerously toxic new frog (Phyllobates) used by Emberá Indians of western Colombia, with discussion of blowgun fabrication and dart poisoning. Bulletin of the AMNH ; v. 161, article 2. (1978).
35. K. C. Pearson, R. D. Tarvin, A review of chemical defense in harlequin toads (Bufonidae: Atelopus). *Toxicon X* **13**, 100092 (2022).
36. B. Hille, *Ion channels of excitable membranes* (Sinauer, 2001).
37. J. W. Daly, Nicotinic Agonists, Antagonists, and Modulators From Natural Sources. *Cell. Mol. Neurobiol.* **25**, 513–552 (2005).
38. M. Stevens, S. Peigneur, J. Tytgat, Neurotoxins and Their Binding Areas on Voltage-Gated Sodium Channels. *Front. Pharmacol.* **2**, 71 (2011).
39. S.-Y. Wang, J. Mitchell, D. B. Tikhonov, B. S. Zhorov, G. K. Wang, How batrachotoxin modifies the sodium channel permeation pathway: computer modeling and site-directed mutagenesis. *Mol. Pharmacol.* **69**, 788–795 (2005).
40. T. Vandendriessche, *et al.*, Modulation of voltage-gated Na+ and K+ channels by pumiliotoxin 251D: A "joint venture" alkaloid from arthropods and amphibians. *Toxicon* **51**, 334–344 (2008).
41. V. M. Bricelj, *et al.*, Sodium channel mutation leading to saxitoxin resistance in clams increases risk of PSP. *Nature* **434**, 763–767 (2005).
42. C. T. Hanifin, The Chemical and Evolutionary Ecology of Tetrodotoxin (TTX) Toxicity in Terrestrial Vertebrates. *Mar. Drugs* **8**, 577–593 (2010).
43. R. D. Tarvin, J. C. Santos, L. A. O'Connell, H. H. Zakon, D. C. Cannatella, Convergent substitutions in a sodium channel suggest multiple origins of toxin resistance in poison frogs. *Mol. Biol. Evol.* **33**, 1068–1081 (2016).
44. O. Torres-Carvajal, K. C. Hinojosa, Hidden diversity in two widespread snake species (Serpentes: Xenodontini: Erythrolamprus) from South America. *Mol. Phylogenet. Evol.* **146**, 106772 (2020).
45. E. D. Cope, *Contributions to the herpetology of New Granada and Argentina, with descriptions of new forms* (the Philadelphia Museums, 1899).
46. B. W. Perry, *et al.*, Molecular Adaptations for Sensing and Securing Prey and Insight into Amniote Genome Diversity from the Garter Snake Genome. *Genome Biol. Evol.* **10**, 2110–2129 (2018).
47. P. M. Vaelli, *et al.*, The skin microbiome facilitates adaptive tetrodotoxin production in poisonous newts. *eLife* **9**, e53898 (2020).
48. J. S. Reimche, *et al.*, The road not taken: Evolution of tetrodotoxin resistance in the Sierra garter snake (Thamnophis couchii) by a path less travelled. *Mol. Ecol.* **31**, 3827–3843 (2022).
49. C. R. Feldman, *et al.*, Is there more than one way to skin a newt? Convergent toxin resistance in snakes is not due to a common genetic mechanism. *Heredity* **116**, 84–91 (2016).
50. H. H. Zakon, Adaptive evolution of voltage-gated sodium channels: The first 800 million years. *Proc. Natl. Acad. Sci.* **109**, 10619–10625 (2012).

51. H. H. Zakon, D. J. Zwickl, Y. Lu, D. M. Hillis, Molecular evolution of communication signals in electric fish. *J. Exp. Biol.* **211**, 1814–1818 (2008).
52. H. Terlau, *et al.*, Mapping the site of block by tetrodotoxin and saxitoxin of sodium channel II. *FEBS Lett.* **293**, 93–96 (1991).
53. E. D. Brodie, E. D. Brodie, Tetrodotoxin resistance in garter snakes: an evolutionary response of predators to dangerous prey. *Evolution* **44**, 651–659 (1990).
54. S.-Y. Wang, G. K. Wang, Voltage-gated sodium channels as primary targets of diverse lipid-soluble neurotoxins. *Cell. Signal.* **15**, 151–159 (2003).
55. J. E. Fux, A. Mehta, J. Moffat, J. D. Spafford, Eukaryotic Voltage-Gated Sodium Channels: On Their Origins, Asymmetries, Losses, Diversification and Adaptations. *Front. Physiol.* **9** (2018).
56. M. Vornanen, M. Hassinen, J. Haverinen, Tetrodotoxin Sensitivity of the Vertebrate Cardiac Na+ Current. *Mar. Drugs* **9**, 2409–2422 (2011).
57. W. L. Eckalbar, *et al.*, Genome reannotation of the lizard Anolis carolinensis based on 14 adult and embryonic deep transcriptomes. *BMC Genomics* **14**, 49 (2013).
58. M. Amano, T. Takatani, F. Sakayauchi, R. Oi, Y. Sakakura, The brain of the wild toxic marine pufferfishes accumulates tetrodotoxin. *Toxicon* **218**, 1–7 (2022).
59. K. L. Gendreau, *et al.*, Sex linkage of the skeletal muscle sodium channel gene (SCN4A) explains apparent deviations from Hardy–Weinberg equilibrium of tetrodotoxin-resistance alleles in garter snakes (Thamnophis sirtalis). *Heredity* **124**, 647–657 (2020).
60. J. W. Daly, F. Gusovsky, C. W. Myers, M. Yotsu-Yamashita, T. Yasumoto, First occurrence of tetrodotoxin in a dendrobatid frog (Colostethus inguinalis), with further reports for the bufonid genus Atelopus. *Toxicon* **32**, 279–285 (1994).
61. T. Grant, On the identities of Colostethus inguinalis (Cope, 1868) and C. panamensis (Dunn, 1933), with comments on C. latinasus (Cope, 1863) (Anura, Dendrobatidae). American Museum novitates ; no. 3444. *Identities of Colostethus inguinalis (Cope, 1868) and C. panamensis (Dunn, 1933).* (2004).
62. E. La Marca, *et al.*, Catastrophic Population Declines and Extinctions in Neotropical Harlequin Frogs (Bufonidae: Atelopus)1. *Biotropica* **37**, 190–201 (2005).
63. S. Lötters, *et al.*, Ongoing harlequin toad declines suggest the amphibian extinction crisis is still an emergency. *Commun. Earth Environ.* **4**, 1–8 (2023).
64. T. Grant, A new, toxic species of Colostethus (Anura: Dendrobatidae: Colostethinae) from the Cordillera Central of Colombia. *Zootaxa* **1555**, 39–51 (2007).
65. C. Martin H., *et al.*, Metabolites from Microbes Isolated from the Skin of the Panamanian Rocket Frog Colostethus panamansis (Anura: Dendrobatidae). *Metabolites* **10**, 406 (2020).
66. A. N. Stokes, *et al.*, Confirmation and distribution of tetrodotoxin for the first time in terrestrial invertebrates: Two terrestrial flatworm species (Bipalium adventitium and Bipalium kewense). *PLoS ONE* **9**, e100718 (2014).
67. E. J. Britt, A. F. Bennett, The Energetic Advantages of Slug Specialization in Garter Snakes (Genus Thamnophis). *Physiol. Biochem. Zool.* **81**, 247–254 (2008).
68. S. J. Arnold, Polymorphism and Geographic Variation in the Feeding Behavior of the Garter Snake Thamnophis elegans. *Science* **197**, 676–678 (1977).
69. G. M. Lipkind, H. A. Fozzard, A structural model of the tetrodotoxin and saxitoxin binding site of the Na+ channel. *Biophys. J.* **66**, 1–13 (1994).
70. D. Colquhoun, R. Henderson, J. M. Ritchie, The binding of labelled tetrodotoxin to non-myelinated nerve fibres. *J. Physiol.* **227**, 95–126 (1972).
71. M.-M. Zhang, *et al.*, Synergistic and Antagonistic Interactions between Tetrodotoxin and μ-Conotoxin in Blocking Voltage-gated Sodium Channels. *Channels Austin Tex* **3**, 32–38 (2009).
72. J. W. Daly, *et al.*, Pumiliotoxin alkaloids: a new class of sodium channel agents. *Biochem. Pharmacol.* **40**, 315–326 (1990).
73. F. Gusovsky, W. L. Padgett, C. R. Creveling, J. W. Daly, Interaction of pumiliotoxin B with an “alkaloid-binding domain”; on the voltage-dependent sodium channel. *Mol. Pharmacol.*

42, 1104–1108 (1992).
74. T. Lovenberg, J. W. Daly, Histrionicotoxins: effects on binding of radioligands for sodium, potassium, and calcium channels in brain membranes. *Neurochem. Res.* **11**, 1609–1621 (1986).
75. S. Mohammadi, *et al.*, Constraints on the evolution of toxin-resistant Na,K-ATPases have limited dependence on sequence divergence. *PLOS Genet.* **18**, e1010323 (2022).
76. B. D. Bitarello, D. Y. C. Brandt, D. Meyer, A. M. Andrés, Inferring Balancing Selection From Genome-Scale Data. *Genome Biol. Evol.* **15**, evad032 (2023).
77. T. R. Booker, B. C. Jackson, P. D. Keightley, Detecting positive selection in the genome. *BMC Biol.* **15**, 98 (2017).
78. D. R. Schield, *et al.*, The roles of balancing selection and recombination in the evolution of rattlesnake venom. *Nat. Ecol. Evol.* **6**, 1367–1380 (2022).
79. E. D. Brodie, B. J. Ridenhour, E. D. Brodie, The evolutionary response of predators to dangerous prey: Hotspots and coldspots in the geographic mosaic of coevolution between garter snakes and newts. *Evolution* **56**, 2067–2082 (2002).
80. R. E. del Carlo, *et al.*, Coevolution with toxic prey produces functional trade-offs in sodium channels of predatory snakes. *eLife* **13** (2024).
81. J. D. Lynch, P. M. Ruiz-Carranza, M. C. Ardila-Robayo, Biogeographic patterns of Colombian frogs and toads (Patrones biogeográficos de las ranas y los sapos de Colombia). *Rev. Acad. Colomb. Cienc. Exactas Físicas Nat.* **21**, 237–248 (1997).
82. C. T. Hanifin, W. F. Gilly, Evolutionary history of a complex adaptation: Tetrodotoxin resistance in salamanders. *Evolution* **69**, 232–244 (2015).
83. S. Andrews, FastQC: A Quality Control tool for High Throughput Sequence Data. (2010). Deposited 2010.
84. A. M. Bolger, M. Lohse, B. Usadel, Trimmomatic: a flexible trimmer for Illumina sequence data. *Bioinformatics* **30**, 2114–2120 (2014).
85. Picard toolkit. *Broad Inst. GitHub Repos.* (2019).
86. P. Danecek, *et al.*, Twelve years of SAMtools and BCFtools. *GigaScience* **10**, giab008 (2021).
87. R. D. Finn, J. Clements, S. R. Eddy, HMMER web server: interactive sequence similarity searching. *Nucleic Acids Res.* **39**, W29–W37 (2011).
88. A. R. Quinlan, I. M. Hall, BEDTools: A flexible suite of utilities for comparing genomic features. *Bioinformatics* **26**, 841–842 (2010).
89. S. F. Altschul, W. Gish, W. Miller, E. W. Myers, D. J. Lipman, Basic local alignment search tool. *J. Mol. Biol.* **215**, 403–410 (1990).
90. J. W. McGlothlin, *et al.*, Parallel evolution of tetrodotoxin resistance in three voltage-gated sodium channel genes in the garter snake thamnophis sirtalis. *Mol. Biol. Evol.* **31**, 2836–2846 (2014).
91. M. A. Miller, W. Pfeiffer, T. Schwartz, Creating the CIPRES Science Gateway for inference of large phylogenetic trees in *2010 Gateway Computing Environments Workshop (GCE)*, (2010), pp. 1–8.
92. L.-T. Nguyen, H. A. Schmidt, A. von Haeseler, B. Q. Minh, IQ-TREE: A Fast and Effective Stochastic Algorithm for Estimating Maximum-Likelihood Phylogenies. *Mol. Biol. Evol.* **32**, 268–274 (2015).
93. I. Letunic, P. Bork, Interactive Tree Of Life (iTOL) v5: an online tool for phylogenetic tree display and annotation. *Nucleic Acids Res.* **49**, W293–W296 (2021).
94. S. S. Garber, C. Miller, Single Na+ channels activated by veratridine and batrachotoxin. *J. Gen. Physiol.* **89**, 459–480 (1987).
95. S. L. Kosakovsky Pond, *et al.*, HyPhy 2.5—A Customizable Platform for Evolutionary Hypothesis Testing Using Phylogenies. *Mol. Biol. Evol.* **37**, 295–299 (2019).
96. C. P. Meyer, Molecular systematics of cowries (Gastropoda: Cypraeidae) and diversification patterns in the tropics. *Biol. J. Linn. Soc.* **79**, 401–459 (2003).
97. S. Palumbi, A. Martin, S. Romano, G. Grabowski, Simple Fool's Guide THE SIMPLE FOOL'S GUIDE TO PCR. (2002).

98. K. D. Yamada, K. Tomii, K. Katoh, Application of the MAFFT sequence alignment program to large data—reexamination of the usefulness of chained guide trees. *Bioinformatics* **32**, 3246–3251 (2016).
99. C. Zhang, M. Rabiee, E. Sayyari, S. Mirarab, ASTRAL-III: polynomial time species tree reconstruction from partially resolved gene trees. *BMC Bioinformatics* **19**, 153 (2018).
100. T.-K. Seo, Calculating Bootstrap Probabilities of Phylogeny Using Multilocus Sequence Data. *Mol. Biol. Evol.* **25**, 960–971 (2008).
101. B. Murrell, *et al.*, Detecting Individual Sites Subject to Episodic Diversifying Selection. *PLOS Genet.* **8**, e1002764 (2012).
102. S. Weaver, *et al.*, Datamonkey 2.0: A Modern Web Application for Characterizing Selective and Other Evolutionary Processes. *Mol. Biol. Evol.* **35**, 773–777 (2018).
103. S. Pond, MEME analysis result visualization. *Observable* (2020). Available at: https://observablehq.com/@spond/meme [Accessed 21 March 2023].
104. J. W. Leigh, D. Bryant, popart: full-feature software for haplotype network construction. *Methods Ecol. Evol.* **6**, 1110–1116 (2015).
105. E. Paradis, pegas: an R package for population genetics with an integrated–modular approach. *Bioinformatics* **26**, 419–420 (2010).
106. H. Wickham, *ggplot2: Elegant Graphics for Data Analysis* (Springer International Publishing, 2009).
107. C. Sievert, *Interactive Web-Based Data Visualization with R, plotly, and shiny* (Chapman and Hall/CRC, 2020).
108. D. Vázquez-Restrepo, CalPhotos: Erythrolamprus epinephalus. (2019). Available at: https://calphotos.berkeley.edu/cgi/img_query?enlarge=0000+0000+0519+1034 [Accessed 13 March 2023].

Figures

Figure 1. Methodology to screen for amino acid sites involved in target-site resistance (TSR) and identify putative TSR positions in *E. reginae* and *E. epinephelus*. A) Target sequencing was employed to enrich and sequence the voltage-gated sodium channel (VGSC) genes (dark grey) from Colombian snake species. The resulting reads were mapped to VGSCs in the *Python guttatus* genome (light blue). These reads were then BLASTed against *Thamnophis sirtalis* VGSC exons (red lines), enabling us to assemble partial or complete VGSCs from the focal species. Sequences from all VGSC genes and samples were aligned. Using this VGSC family alignment, we applied three specific conditions to identify putative TSR positions (see Putative TSR positions step). If a position met all three conditions, the amino acid change (star) was characterized as a putative TSR position (red star and circle; position 1, "P1"); if not, it was not selected (grey star). B) Unfolded two-dimensional VGSC structural representation. Six transmembrane segments (S1 – S6), the pore (S5 – S6) and one extracellular p-loop are found in each of four domains (DI – DIV). The nine amino acid positions of interest are highlighted in circles with the corresponding position number (e.g. P1 in DI-S6). Positions known to provide TTX resistance are highlighted by the level of toxicity: P4 and P6 exhibit moderate TTX and STX resistance (grey circles) (1, 47, 52). P7 and P8 confer extreme TTX resistance (black circles) (1).

Figure 2. A representative set of amino acid changes in nine homologous sites identified in eight VGSC genes in *Erythrolamprus reginae*, *E. epinephelus,* and *E.* sp. samples. In many cases, each species included individuals with haplotypes encoding a non-resistant variant (“NR”) that is similar to the outgroup sequence as well as one or multiple haplotypes with non-synonymous substitutions assigned as possible “resistant” variants (“R”). Additional singleton changes that we identified in these regions are visualized in Dataset S1B. For comparison, we include haplotypes

from *Thamnophis sirtalis*, a relatively TTX-resistant snake (Genbank numbers in Table S4). The reference sequence corresponds to an ancestral reconstruction of the snake Most Recent Common Ancestor (snake MCRA). The positions of interest (P1-P9) are highlighted in orange. Substitutions that showed evidence of positive, diversifying selection under the Mixed Effects Model of Evolution, MEME, (likelihood-ratio test (LRT) p <0.07) are highlighted in purple text. TTX-resistance-related positions are highlighted in grey by the level of toxicity (see Fig. 1 for legend).

Figure 3. Geographic and phylogenetic distribution of samples in this study. A) Phylogenetic tree based on two mitochondrial genes (*COI*, *16S*) and two nuclear genes (*RAG2* and *c-mos*), alongside a map of the *Erythrolamprus* samples. Bootstrapping is shown for each node. *E. reginae* samples are represented in the map as circles: Amazonia, black; Guaviare, white; Boyacá, grey. Given that our samples of *E. epinephelus* formed two groups, we divided samples into two groups: Group 1 represented as triangles (G1), and group 2 as squares (G2). The distributional range of *E. reginae* is shown in purple and *E. epinephelus* in red. *E. reginae* photo from Leticia, Amazonas, courtesy of Dario Alarcón Naforo; *E. epinephelus* photo from Caldas, Antioquía, courtesy of Daniel Vásquez-Restrepo via CalPhotos with license CC BY-NC-SA 3.0 © 2019 (108). Neither of the photos corresponds to the samples used in this study. B) The presence and distribution of the identified TTX-resistant changes from positions P4 (moderate TTX resistance), P6 (moderate TTX resistance), and P7 and P8 (both extreme TTX resistance) in the *Erythrolamprus* genus samples. Fully filled circles represent the presence of a particular substitution in all individuals of that species. Half-filled circles represent sites where the amino acid change is not present across all individuals of that species (this only applies to species with more than one sample: *E. melanotus*, *E. reginae* and *E. epinephelus*).

Figure 4. Summary of the nine positions identified in this study as potential TSR-conferring sites for *Erythrolamprus reginae* and *E. epinephelus*. From the outer to the inner circle, we summarized for each position P1-P9 the presence of each amino acid change across the 8 *E. reginae* individuals and 9 *E. epinephelus* individuals (Presence), the amino acid change and position with *Mus musculus* gene annotation (AA change), the gene(s) where this change was found (Gene), and the evidence for toxin resistance in previous literature or presence in other toxin-resistant organisms (Evidence). Genes, changes, and presence of alleles are color-coded using the same color scheme as in Fig. 3B and Fig. 5. According to the legend in Fig. 1, we highlighted in grey (P4 and P6) and black (P7 and P8) the TTX resistant positions. Ind., individual.

Figure 5. Haplotype diversity for positions P7 and P8 and domain IV (DIV) haplotype network for *Erythrolamprus reginae* and *E. epinephelus* samples. A) Phylogenetic tree used in Fig. 3A highlighting the *Erythrolamprus* genus samples with a visual representation of the P7 and P8 haplotypes for the VGSC genes. The amino acid "DG" is considered a non-resistant genotype in these groups (white transparent amino acid codes). Resistant haplotypes found in homozygosis are shown in red and resistant haplotypes that occur in heterozygosis with the non-resistant haplotype are shown in orange. Colors at the bottom of the alignment correspond to amino acid changes in Figs. 3B and 4. B) DIV haplotype networks for *E. reginae* and *E. epinephelus*. The legend shows the nucleotides that encode the amino acid variants from each haplotype at P7 and P8 positions. Non-resistant amino acid and nucleotide variants are shown in black and resistant variants in red. Standardized size of a circle that represents 1 or 10 haplotypes is shown on the left. Fill colors of circles correspond to amino acid changes that may provide TTX resistance, as also shown in panel A of this figure, Fig. 3B, and Fig. 4.

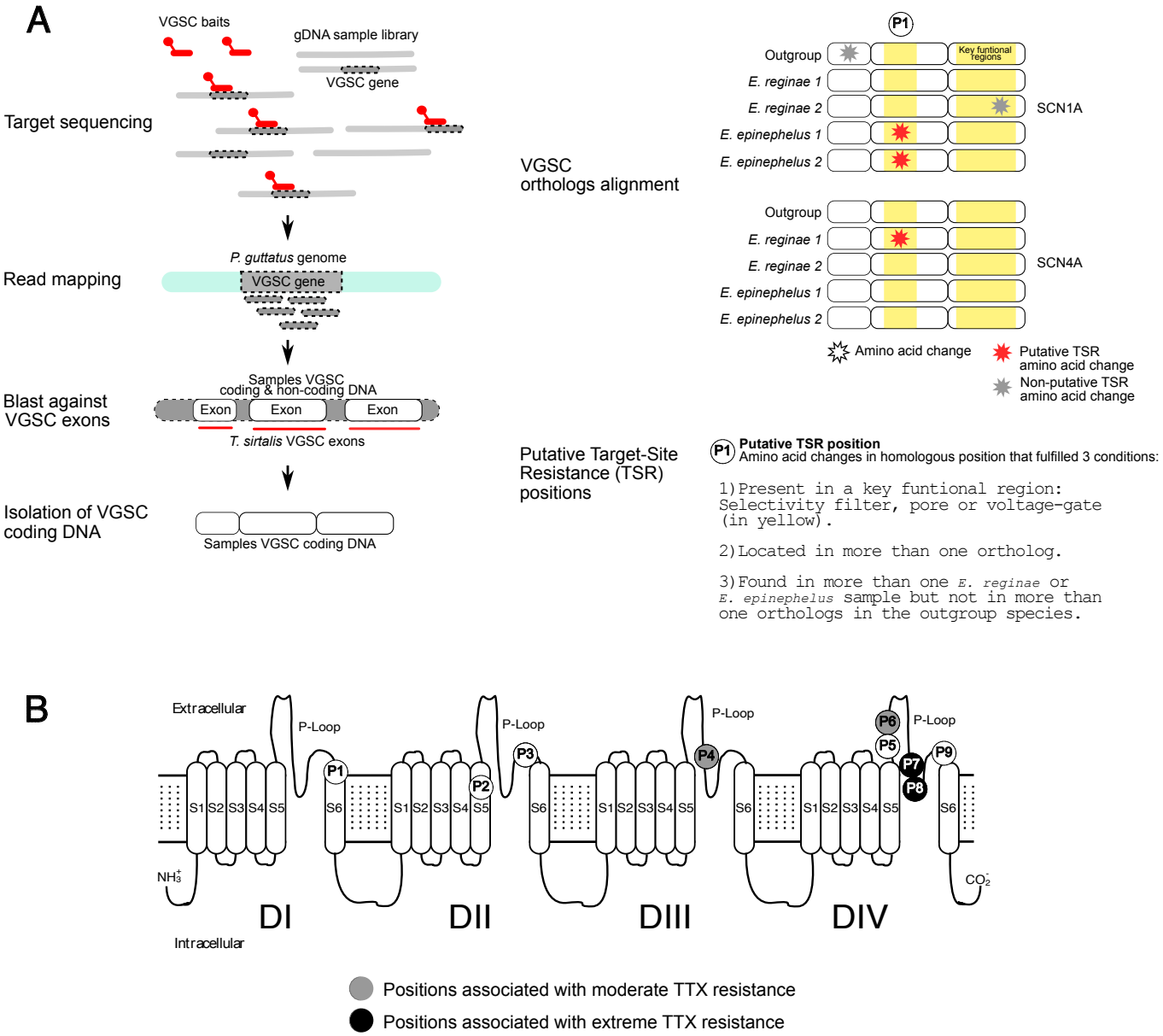
A
VGSC baits
gDNA sample library
VGSC gene
Target sequencing
P. guttatus genome
VGSC gene
Read mapping
Samples VGSC
coding & non-coding DNA
Exon
Exon
Exon
T. sirtalis VGSC exons
Blast against
VGSC exons
Isolation of VGSC
coding DNA
Samples VGSC coding DNA
VGSC
orthologs alignment
P1
Key funtional regions
Outgroup
E. reginae 1
E. reginae 2
E. epinephelus 1
E. epinephelus 2
SCN1A
Outgroup
E. reginae 1
E. reginae 2
E. epinephelus 1
E. epinephelus 2
SCN4A
Amino acid change
Putative TSR
amino acid change
Non-putative TSR
amino acid change
Putative Target-Site
Resistance (TSR)
positions
P1 Putative TSR position
Amino acid changes in homologous position that fulfilled 3 conditions:
1) Present in a key funtional region:
Selectivity filter, pore or voltage-gate
(in yellow).
2) Located in more than one ortholog.
3) Found in more than one E. reginae or
E. epinephelus sample but not in more than
one orthologs in the outgroup species.

B
Extracellular
P-Loop
P-Loop
P-Loop
P-Loop
P1
P2
P3
P4
P5
P6
P7
P8
P9
S1 S2 S3 S4 S5
S6
NH3+
CO2-
DI
DII
DIII
DIV
Intracellular
Positions associated with moderate TTX resistance
Positions associated with extreme TTX resistance

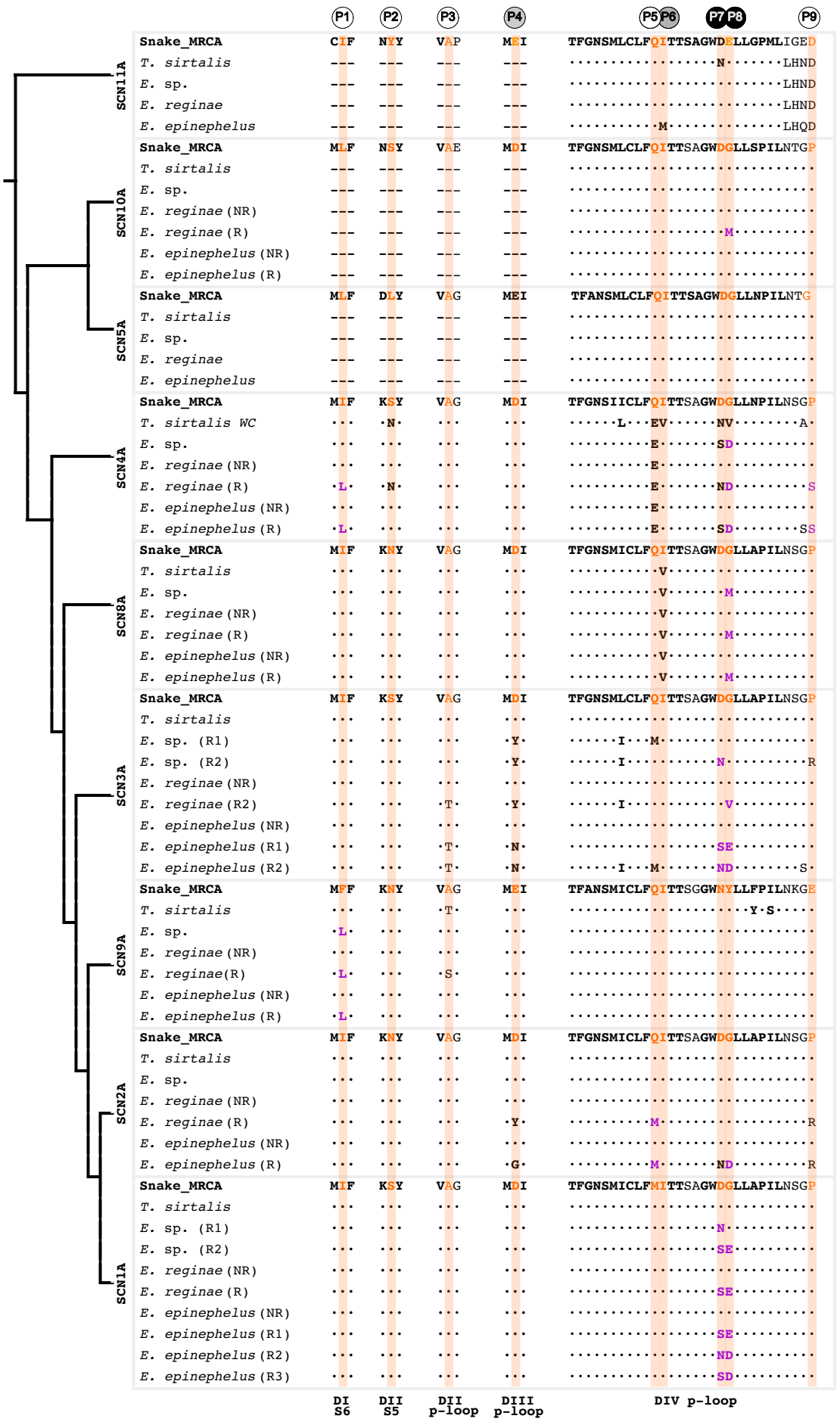
P1 P2 P3 P4 P5 P6 P7 P8 P9
SCN11A
Snake_MRCA CIF NYY VAP MEI TFGNSMLCLFQITTSAGWDELLGPMLIGED
T. sirtalis ··· ··· ··· ··· ··········N·····LHND
E. sp. ··· ··· ··· ··· ··········LHND
E. reginae ··· ··· ··· ··· ··········LHND
E. epinephelus ··· ··· ··· ··· ··M·····LHQD
SCN10A
Snake_MRCA MLF NSY VAE MDI TFGNSMLCLFQITTSAGWDGLLSPILNTGP
T. sirtalis ··· ··· ··· ··· ··········
E. sp. ··· ··· ··· ··· ··········
E. reginae (NR) ··· ··· ··· ··· ··········
E. reginae (R) ··· ··· ··· ··· ··········M·····
E. epinephelus (NR) ··· ··· ··· ··· ··········
E. epinephelus (R) ··· ··· ··· ··· ··········
SCN5A
Snake_MRCA MLF DLY VAG MEI TFANSMLCLFQITTSAGWDGLLNPILNTG
T. sirtalis ··· ··· ··· ··· ··········
E. sp. ··· ··· ··· ··· ··········
E. reginae ··· ··· ··· ··· ··········
E. epinephelus ··· ··· ··· ··· ··········
SCN4A
Snake_MRCA MIF KSY VAG MDI TFGNSIICLFQITTSAGWDGLLNPILNSGP
T. sirtalis WC ···· ·N· ··· ··· ·····L···EV·····NV·····A·
E. sp. ··· ··· ··· ··· ··········E·····SD·····
E. reginae (NR) ··· ··· ··· ··· ··········E·····
E. reginae (R) ·L· ·N· ··· ··· ··········E·····ND·····S
E. epinephelus (NR) ··· ··· ··· ··· ··········E·····
E. epinephelus (R) ·L· ··· ··· ··· ··········E·····SD·····SS
SCN8A
Snake_MRCA MIF KNY VAG MDI TFGNSMICLFQITTSAGWDGLLAPILNSGP
T. sirtalis ··· ··· ··· ··· ··········V·····
E. sp. ··· ··· ··· ··· ··········V·····M·····
E. reginae (NR) ··· ··· ··· ··· ··········V·····
E. reginae (R) ··· ··· ··· ··· ··········V·····M·····
E. epinephelus (NR) ··· ··· ··· ··· ··········V·····
E. epinephelus (R) ··· ··· ··· ··· ··········V·····M·····
SCN3A
Snake_MRCA MIF KSY VAG MDI TFGNSMLCLFQITTSAGWDGLLAPILNSGP
T. sirtalis ··· ··· ··· ··· ··········
E. sp. (R1) ··· ··· ··· ·Y· ·····I···M·····
E. sp. (R2) ··· ··· ··· ·Y· ·····I··········N·····R
E. reginae (NR) ··· ··· ··· ··· ··········
E. reginae (R2) ··· ··· ·T· ·Y· ·····I··········V·····
E. epinephelus (NR) ··· ··· ··· ··· ··········
E. epinephelus (R1) ··· ··· ·T· ·N· ··········SE·····
E. epinephelus (R2) ··· ··· ·T· ·N· ·····I···M·····ND·····S·
SCN9A
Snake_MRCA MFF KNY VAG MEI TFANSMICLFQITTSGGWNYLLFPILNKGE
T. sirtalis ··· ··· ·T· ··· ··········Y·S·····
E. sp. ·L· ··· ··· ··· ··········
E. reginae (NR) ··· ··· ··· ··· ··········
E. reginae (R) ·L· ··· ·S· ··· ··········
E. epinephelus (NR) ··· ··· ··· ··· ··········
E. epinephelus (R) ·L· ··· ··· ··· ··········
SCN2A
Snake_MRCA MIF KNY VAG MDI TFGNSMICLFQITTSAGWDGLLAPILNSGP
T. sirtalis ··· ··· ··· ··· ··········
E. sp. ··· ··· ··· ··· ··········
E. reginae (NR) ··· ··· ··· ··· ··········
E. reginae (R) ··· ··· ··· ·Y· ··········M·····R
E. epinephelus (NR) ··· ··· ··· ··· ··········
E. epinephelus (R) ··· ··· ··· ·G· ··········M·····ND·····R
SCN1A
Snake_MRCA MIF KSY VAG MDI TFGNSMICLFMITTSAGWDGLLAPILNSGP
T. sirtalis ··· ··· ··· ··· ··········
E. sp. (R1) ··· ··· ··· ··· ··········N·····
E. sp. (R2) ··· ··· ··· ··· ··········SE·····
E. reginae (NR) ··· ··· ··· ··· ··········
E. reginae (R) ··· ··· ··· ··· ··········SE·····
E. epinephelus (NR) ··· ··· ··· ··· ··········
E. epinephelus (R1) ··· ··· ··· ··· ··········SE·····
E. epinephelus (R2) ··· ··· ··· ··· ··········ND·····
E. epinephelus (R3) ··· ··· ··· ··· ··········SD·····
DI S6
DII S5
DII p-loop
DIII p-loop
DIV p-loop

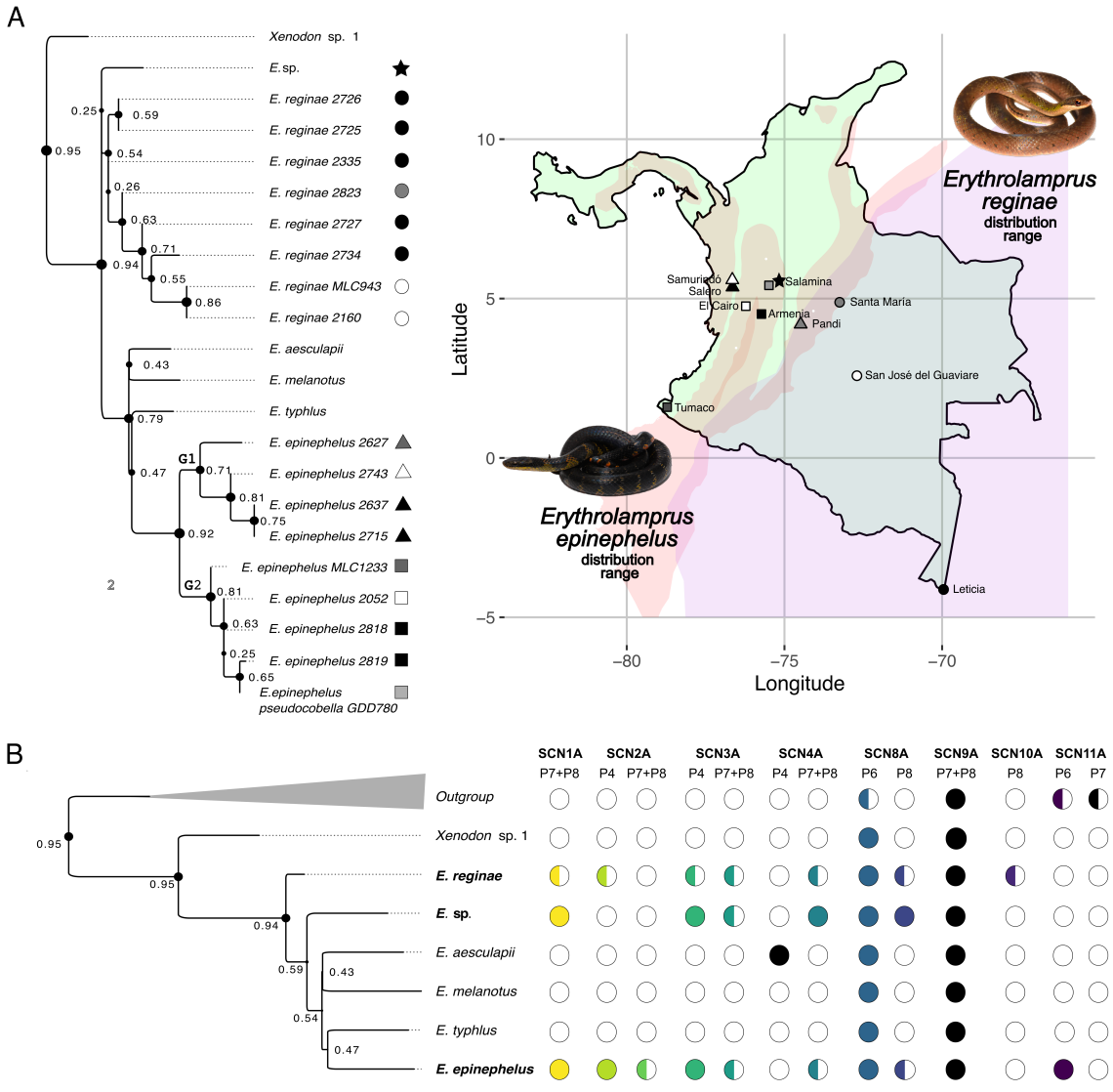
A
Xenodon sp. 1
E. sp.
E. reginae 2726
E. reginae 2725
E. reginae 2335
E. reginae 2823
E. reginae 2727
E. reginae 2734
E. reginae MLC943
E. reginae 2160
E. aesculapii
E. melanotus
E. typhlus
E. epinephelus 2627
E. epinephelus 2743
E. epinephelus 2637
E. epinephelus 2715
E. epinephelus MLC1233
E. epinephelus 2052
E. epinephelus 2818
E. epinephelus 2819
E.epinephelus pseudocobella GDD780
G1
G2
2
0.25
0.59
0.95
0.54
0.26
0.63
0.71
0.94
0.55
0.86
0.43
0.79
0.47
0.71
0.81
0.75
0.92
0.81
0.63
0.25
0.65
Erythrolamprus reginae distribution range
Erythrolamprus epinephelus distribution range
Samuriado
Salero
El Cairo
Salamina
Armenia
Pandi
Santa María
San José del Guaviare
Tumaco
Leticia
Latitude
Longitude
10
5
0
−5
−80
−75
−70
B
SCN1A P7+P8
SCN2A P4 P7+P8
SCN3A P4 P7+P8
SCN4A P4 P7+P8
SCN8A P6 P8
SCN9A P7+P8
SCN10A P8
SCN11A P6 P7
Outgroup
Xenodon sp. 1
E. reginae
E. sp.
E. aesculapii
E. melanotus
E. typhlus
E. epinephelus
0.95
0.95
0.94
0.59
0.43
0.54
0.47

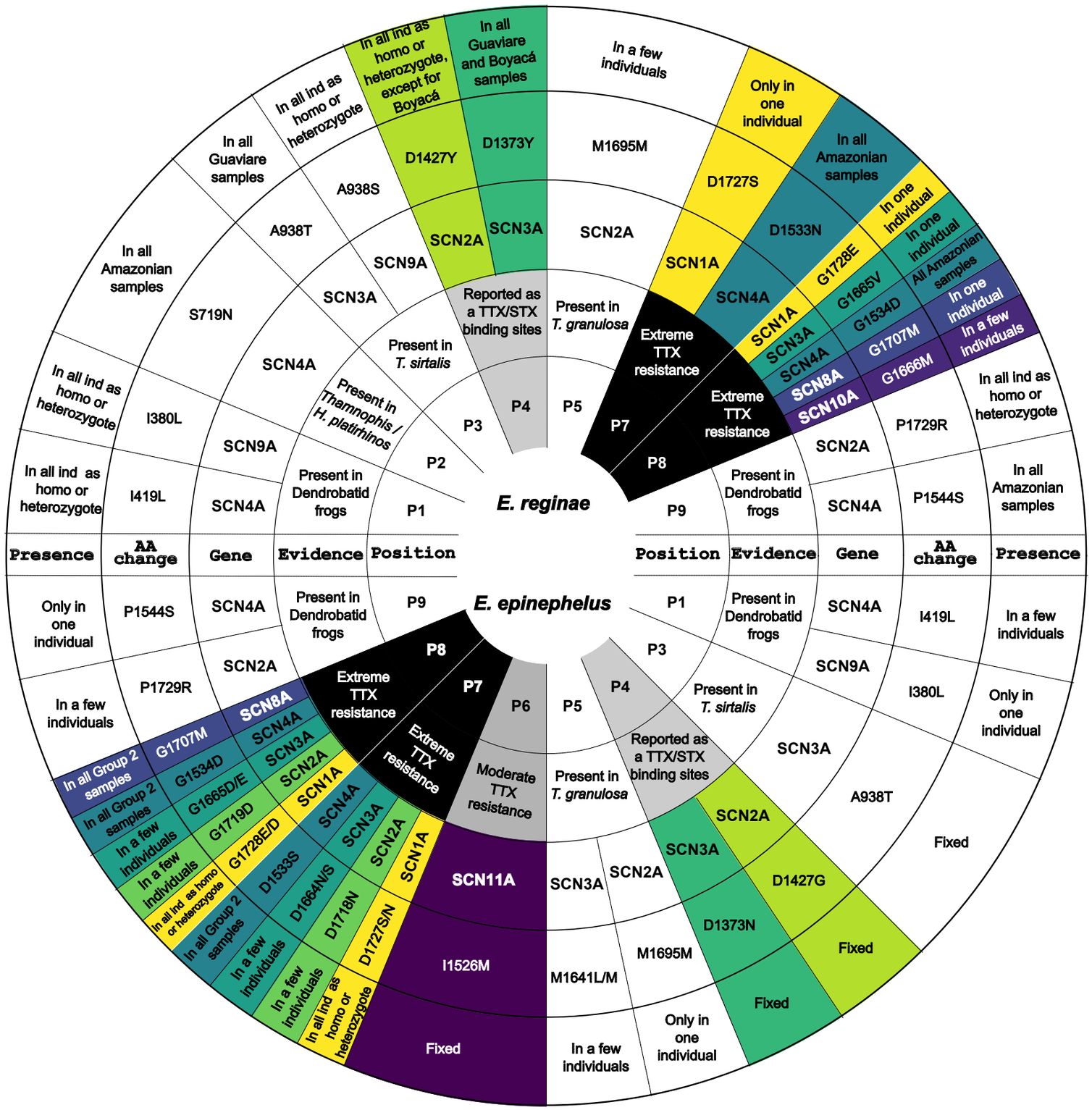
E. reginae
Position
Evidence
Gene
AA change
Presence
P1
Present in Dendrobatid frogs
SCN4A
I419L
In all Amazonian samples
P2
Present in Thamnophis / H. platirhinos
SCN9A
I380L
In all ind as homo or heterozygote
P3
Present in T. sirtalis
SCN3A
A938T
In all Amazonian samples
P4
Reported as a TTX/STX binding sites
SCN2A
D1427Y
In all ind as homo or heterozygote, except for Boyacá
P5
Present in T. granulosa
SCN1A
D1727S
In a few individuals
P7
Extreme TTX resistance
SCN4A
D1533N
In all Amazonian samples
P8
Extreme TTX resistance
SCN1A
G1728E
In one individual
P9
Present in Dendrobatid frogs
SCN2A
P1729R
In all ind as homo or heterozygote
E. epinephelus
Position
Evidence
Gene
AA change
Presence
P1
Present in Dendrobatid frogs
SCN4A
I419L
In a few individuals
P3
Present in T. sirtalis
SCN9A
I380L
Only in one individual
P4
Reported as a TTX/STX binding sites
SCN3A
A938T
Fixed
P5
Present in T. granulosa
SCN2A
P1729R
In a few individuals
P6
Moderate TTX resistance
SCN11A
I1526M
Fixed
P7
Extreme TTX resistance
SCN4A
D1373N
Fixed
P8
Extreme TTX resistance
SCN3A
D1727S/N
In all ind as homo or heterozygote
P9
Present in Dendrobatid frogs
SCN2A
D1427G
In a few individuals
SCN1A
D1373Y
In all Guaviare and Boyacá samples
SCN2A
M1695M
In a few individuals
SCN3A
D1664N/S
In all Group 2 samples
SCN4A
D1533S
In a few individuals
SCN8A
G1707M
In all Group 2 samples
SCN10A
G1666M
In a few individuals
SCN8A
G1707M
In all Group 2 samples
SCN4A
G1534D
In all Group 2 samples
SCN3A
G1665D/E
In a few individuals
SCN2A
G1719D
In a few individuals
SCN1A
G1728E/D
In all ind as homo or heterozygote
SCN4A
D1533S
In a few individuals
SCN3A
D1664N/S
In a few individuals
SCN2A
D1718N
In all ind as homo or heterozygote
SCN1A
D1727S/N
Fixed
SCN11A
I1526M
Fixed
SCN3A
M1641L/M
In a few individuals
SCN2A
M1695M
Only in one individual
SCN3A
D1427G
Fixed
SCN2A
D1373N
Fixed
SCN1A
G1728E
In one individual
SCN4A
G1665V
In one individual
SCN3A
G1534D
All Amazonian samples
SCN4A
G1707M
In one individual
SCN8A
G1666M
In a few individuals
SCN10A
P1544S
In all ind as homo or heterozygote
SCN2A
P1729R
In all Amazonian samples
SCN4A
P1544S
Only in one individual

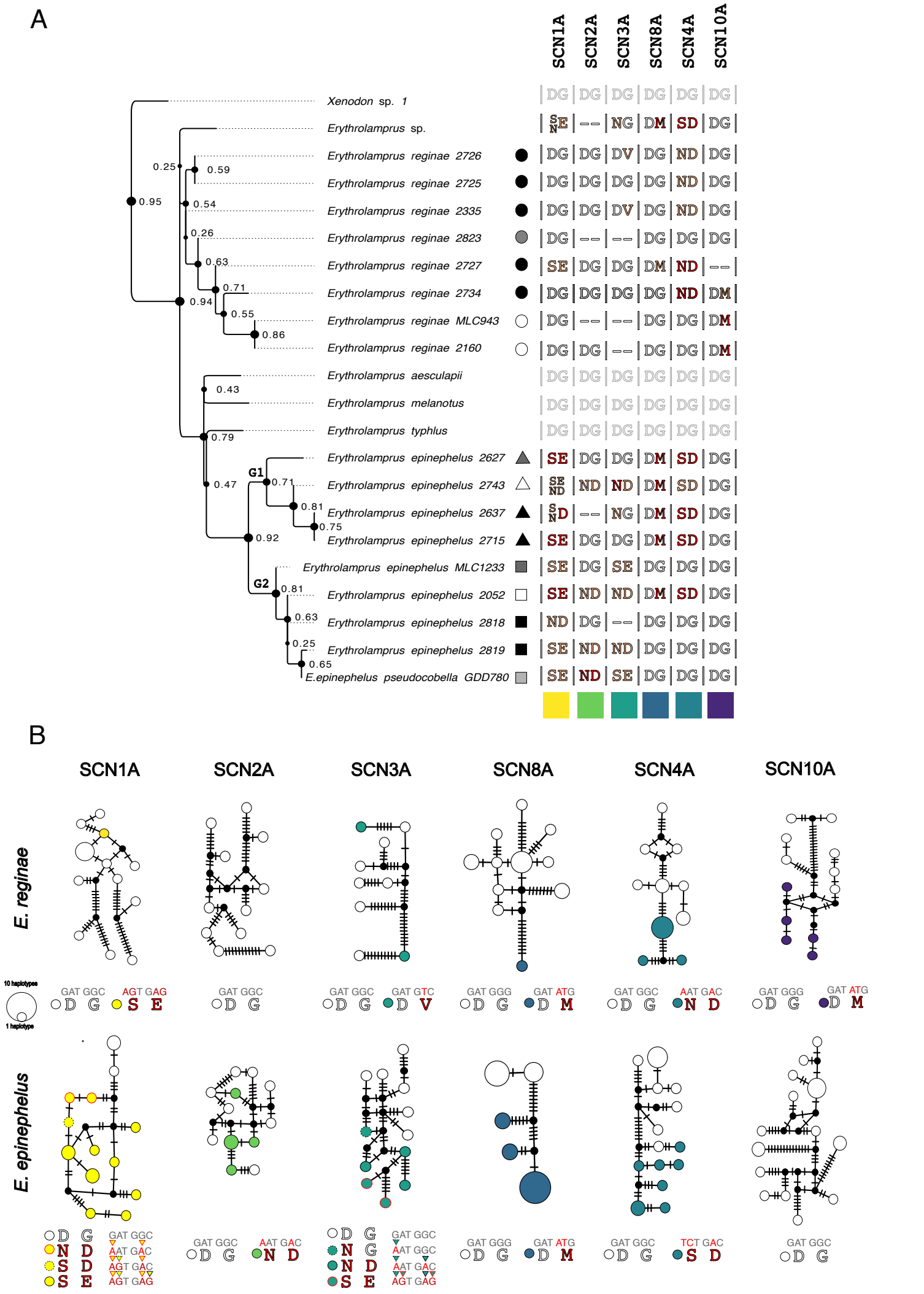
A
SCN1A
SCN2A
SCN3A
SCN8A
SCN4A
SCN10A
Xenodon sp. 1
Erythrolamprus sp.
Erythrolamprus reginae 2726
Erythrolamprus reginae 2725
Erythrolamprus reginae 2335
Erythrolamprus reginae 2823
Erythrolamprus reginae 2727
Erythrolamprus reginae 2734
Erythrolamprus reginae MLC943
Erythrolamprus reginae 2160
Erythrolamprus aesculapii
Erythrolamprus melanotus
Erythrolamprus typhlus
Erythrolamprus epinephelus 2627
Erythrolamprus epinephelus 2743
Erythrolamprus epinephelus 2637
Erythrolamprus epinephelus 2715
Erythrolamprus epinephelus MLC1233
Erythrolamprus epinephelus 2052
Erythrolamprus epinephelus 2818
Erythrolamprus epinephelus 2819
E.epinephelus pseudocobella GDD780
0.25
0.59
0.95
0.54
0.26
0.63
0.71
0.94
0.55
0.86
0.43
0.79
G1
0.47
0.71
0.81
0.75
0.92
G2
0.81
0.63
0.25
0.65
B
SCN1A
SCN2A
SCN3A
SCN8A
SCN4A
SCN10A
E. reginae
E. epinephelus
10 haplotypes
1 haplotype
GAT GGC
AGT GAG
GAT GTC
GAT GGG
GAT ATG
AAT GAC
TCT GAC

Supporting Information for

Predators with a complex toxic diet show a concerted Voltage-Gated Sodium Channel evolution (*Erythrolamprus* sp.)

Valeria Ramírez-Castañeda[1,2,*]; Rebecca D. Tarvin[1,2]; Roberto Marquéz[3]

[1]Museum of Vertebrate Zoology, University of California, Berkeley, CA, 94720
[2]Department of Integrative Biology, University of California, Berkeley, CA, 94720
[3]Department of Biological Sciences, Virginia Tech, Blacksburg, VA 24060

*Valeria Ramírez-Castañeda
Email: vramirezc@berkeley.edu

This PDF file includes:

Supporting text
Figures S1 to S4
Tables S1 to S7
SI References

Other supporting materials for this manuscript include the following:

Datasets S1 to S3

Supporting Text

Supplementary Results

VGSC Sequence Assembly and Phylogenetic Tree Reconstruction

We sequenced the VGSC family of 8 *Erythrolamprus reginae* samples from different 3 localities and 9 *E. epinephelus* samples from 7 localities. We analyzed 40 samples of 21 snake species that coexist in the same habitats, including 25 individuals corresponding to six species of the *Erythrolamprus* genus: *E. aesculapii*, *E. typhlus*, *E. melanotus*, *E. reginae*, *E. epinephelus,* and one individual designated as *Erythrolamprus* sp. that was previously identified as *Erythrolamprus epinephelus* but according to our phylogeny corresponds to a different species that lives in sympatry with *E. epinephelus* (Fig 3A & Table S1). The phylogeny was reconstructed using two mitochondrial (COI, 16S) and two nuclear (c-mos, RAG2) gene sequences. This tree shows high support for nodes among the families and subfamilies, as well as between *Xenodon* and the *Erythrolamprus* genera (bootstrap value > 0.9) (Fig 3A).

On average, 64% (SD = 13.9%) of the reads from each library mapped to the *P. guttatus* genome, as expected considering the phylogenetic distance between our focal species and *P. guttatus*. However, the successfully aligned reads resulted in an average sequencing coverage of 51.24x (SD = 23.03x) (Table S1), which allowed us to obtain phased haplotype sequences for the VGSC covered regions accurately. We were able to reconstruct the complete or near-complete coding sequence for six of the nine VGSC genes found in snakes (*SCN1A, SCN2A, SCN3A, SCN4A, SCN8A, SCN9A*) in all targeted species, as well as Domain IV sequences for the remaining three

(*SCN5A, SCN10A, SCN11A*). In the gene tree, our sequences clustered unambiguously with orthologous sequences and they matched the relationships between paralogs reconstructed in prior studies confirming their correct assembly and annotation (Fig S1) (1–3).

Supplementary Methods

Fig. S4. Methods. Protein match results from *Anolis carolinensis* transcriptome. These results were downloaded from supplementary information in Eckalbar et al., 2013 (4). Nine organ transcriptomes (skin, brain, skeletal muscle, heart, adrenal gland, embryo, lung, ovary, and liver) were used to search for voltage-gated sodium channels using a text finder by typing each of the gene names. Then the number of matches per tissue was plotted using the ggplot package from R (5).

Fig. S1. Voltage-gated Sodium Channel (VGSC) protein family tree. This tree was reconstructed using amino acid sequences in this study and sequences from model vertebrate and reptile species available on GenBank (Table S4). Each color represents one monophyletic group corresponding to a single VGSC protein. From this study, only domain IV (DIV) was retrieved from *SCN5A*, *SCN10A* and *SCN11A*. As reported in the literature, the genes *SCN1A, SCN2A,* and SCN3A in *Xenopus tropicalis* are not homologous to the reptiles and mammals genes and form a monophyletic group (1, 2). Additionally, the *SCN2A* gene was paraphyletic between mammals and reptiles (3). The alignment used to build this tree is found in database S2.

Fig. S2. Alignment of the nine homologous amino acid changes in the VGSC family found as putative TSR sites for *Erythrolamprus reginae*, *Erythrolamprus epinephelus,* and *Erythrolamprus* sp. species. Extract from Fig. S1. VGSC gene tree to show nine positions of interest. Dots represent the same amino acid change as the outgroup highlighted in red for each protein. Below is a consensus sequence showing amino acids >50% conserved in the alignment. Each color represents a monophyletic VGSC protein. Node size depends on the bootstrap values shown in the legend.

Fig. S3. Pairwise Linkage Disequilibrium (LD) for the TTX extreme resistance-conferring substitutions found in P7 and P8. A) LD for *E. epinephelus* substitutions. Each gene and corresponding amino acid change is exhibited for each axis. The values correspond to an *r2* correlation obtained using the *LDscan* function from the *pegas* R package. A higher *r2* is consistent with a higher linkage between the two sites. B) A) LD for *E. reginae* substitutions. Each gene and corresponding amino acid change is exhibited for each axis. The values correspond to an *r2* correlation obtained using the *LDscan* function from the *pegas* R package. A higher *r2* is consistent with a higher linkage between the two sites.

Fig. S4. Number of positive matches for each of the VGSC genes in the expression profile of different *Anolis carolinensis* organs (4). Each VGSC gene is shown in the legend. Data was obtained from published literature (see Supplementary methods).

Table S1. Information from samples used in this study. Species name, ID, locality, coordinates, collected tissue, previous toxic prey reports, number of reads, number of mapped reads, coverage, and alignment rate are included.

Table S2. The list of genes used to design the baits for target sequencing. The name of the gene and protein, organism, length of the sequence, and GenBank reference are included.

Table S3. VGSC gene location in the *Pantherophis guttatus* genome after annotation. In the table, we provide information for Ensembl gene ID, gene ID, gene name in *P. guttatus* GFF file, region name in *P. guttatus* genome, scaffold in *P. guttatus* genome, position in the scaffold, and strand direction. To eliminate the introns from the sequences we used published exon regions and reported in the table the source organism, the number of exons, and the GenBank ID. Finally, we described the exon location in the *P. guttatus* genome exons and the final number of exons obtained in this study.

Table S4. VGSC protein sequence GenBank ID for model vertebrates and reptiles used in the protein tree. Species names and common names are provided. *CACNA1A* was used as an outgroup.

Table S5. List of statistics obtained from haplotype networks for the domain IV of VGSC genes in *E. reginae*, E*. epinephelus,* and *E. melanotus* samples using PopArt (10). Tajima D statistic (TajiD) and the permutation-based p-value for Tajima D (P_tajiD). In addition, the number of segregating sites (segre_sites), π (pi), and the number of parsimonious sites (parsi_sites) is provided.

Table S6. Summary of the nine reported homologous positions and additional sites that are shared with other toxin-resistant organisms. We provided the functional region where the site is located (Region), the number assigned in this study for the position (Position), gene, amino acid change, presence in samples from this study, organisms with substitutions at this site, and the reference for that report (Reference). From the table, [a]Amphibian's *SCN1A*, *SCN2A*, and *SCN3A* are not orthologs for *SCN1A*, *SCN2A,* and *SCN3A* in mammals and reptiles. [b]SCN2A is paraphyletic between reptiles and mammals. Amino acid notations are based on the Mus musculus *SCN2A*, however, this is not homologous to the reptile *SCN2A* ortholog, P4* Reported as a TTX and STX target site from structural models (6), P6** Site reported to confer moderate TTX resistance (7, 8). P7 & P8 ***Site reported to confer extreme TTX resistance (7), and ****Site reported to confer *SCN4A* BTX resistance (9).

Table S7. Summary of the origin of the nine putative TSR positions found in this study for each VGSC gene. The origin was determined using the sequence of the nodes provided by ancestral reconstruction from Hyphy (see Methods).

Dataset S1 (separate file). Excel sheet including all interesting sites found and MEME test results. A) Sheet A, includes all the interesting sites found in segment 4 (S4), S5, S5, and p-loop of the *Erythrolamprus* genus samples. It includes an assigned number for the substitution (Mutation number), the gene name (Gene), the protein name (Protein), the mutation site in the *Mus musculus* protein, if the change was present in another ortholog (shared change in ortholog), orthologs mutation numbers assign for this study, observations. In addition, we included if the change is only found in the *Erythrolamprus* genus, if it is shown in Fig 2, and if it has a P-value <0.07 from the MEME test. Finally, we include information on whether it fulfilled the requirements to be included as a potential TSR in this study. B) Sheet B provides all the MEME matches with p-values <0.1. We included gene, region, amino acid change in *Mus musculus* protein, orthologs

that share this change (Shared in other orthologs), observations if this change is showed in Dataset S1 – Sheet A, if showed in Fig 2, and the p-value obtained from the MEME test.

Dataset S2 (separate file). The amino acid alignment from the VGSC used to reconstruct the protein tree in fasta format (Fig S1 & Table S4).

Dataset S3 (separate file). Phased VGSC gene sequences annotated for this study in fasta format. We only obtained DIV for *SCN5A*, *SCN10A,* and *SCN11A*.

SI References

1. R. L. Rogers, *et al.*, Genomic Takeover by Transposable Elements in the Strawberry Poison Frog. *Mol. Biol. Evol.* **35**, 2913–2927 (2018).
2. K. L. Gendreau, A. D. Hornsby, M. T. J. Hague, J. W. McGlothlin, Gene Conversion Facilitates the Adaptive Evolution of Self-Resistance in Highly Toxic Newts. *Mol. Biol. Evol.* **38**, 4077–4094 (2021).
3. B. J. Liebeskind, D. M. Hillis, H. H. Zakon, Convergence of ion channel genome content in early animal evolution. *Proc. Natl. Acad. Sci. U. S. A.* **112**, 846–851 (2015).
4. W. L. Eckalbar, *et al.*, Genome reannotation of the lizard Anolis carolinensis based on 14 adult and embryonic deep transcriptomes. *BMC Genomics* **14**, 49 (2013).
5. H. Wickham, *ggplot2: Elegant Graphics for Data Analysis* (Springer International Publishing, 2009).
6. H. Terlau, *et al.*, Mapping the site of block by tetrodotoxin and saxitoxin of sodium channel II. *FEBS Lett.* **293**, 93–96 (1991).
7. S. L. Geffeney, E. Fujimoto, E. D. Brodie, E. D. Brodie, P. C. Ruben, Evolutionary diversification of TTX-resistant sodium channels in a predator-prey interaction. *Nature* **434**, 759–763 (2005).
8. P. M. Vaelli, *et al.*, The skin microbiome facilitates adaptive tetrodotoxin production in poisonous newts. *eLife* **9**, e53898 (2020).
9. S.-Y. Wang, G. K. Wang, Point mutations in segment I-S6 render voltage-gated Na+ channels resistant to batrachotoxin. *Proc. Natl. Acad. Sci.* **95**, 2653–2658 (1998).
10. J. W. Leigh, D. Bryant, popart: full-feature software for haplotype network construction. *Methods Ecol. Evol.* **6**, 1110–1116 (2015).

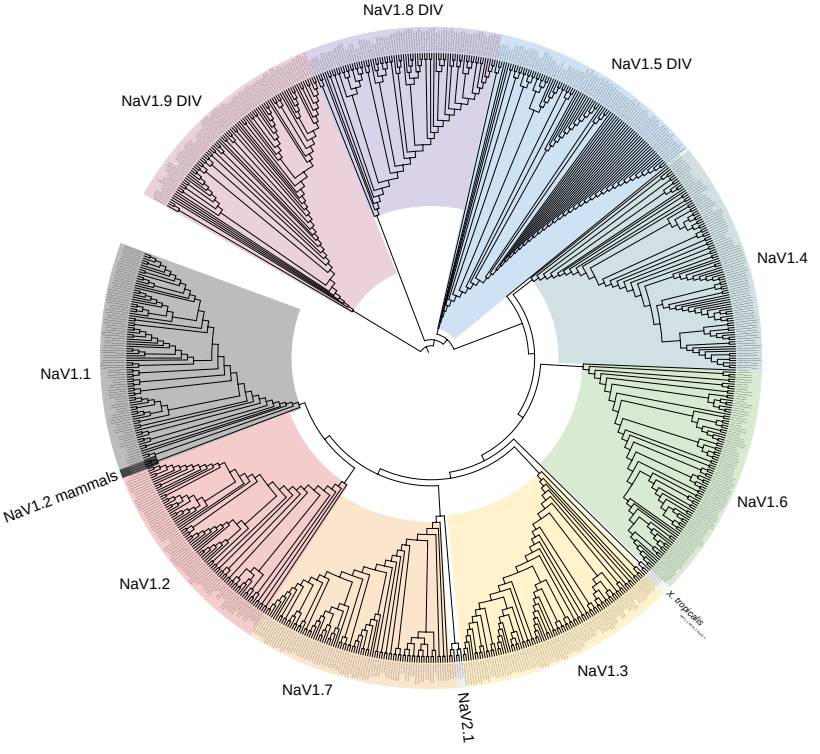
NaV1.8 DIV
NaV1.5 DIV
NaV1.9 DIV
NaV1.4
NaV1.1
NaV1.6
NaV1.2 mammals
NaV1.2
X. tropicalis
NaV1.3
NaV1.7
NaV2.1

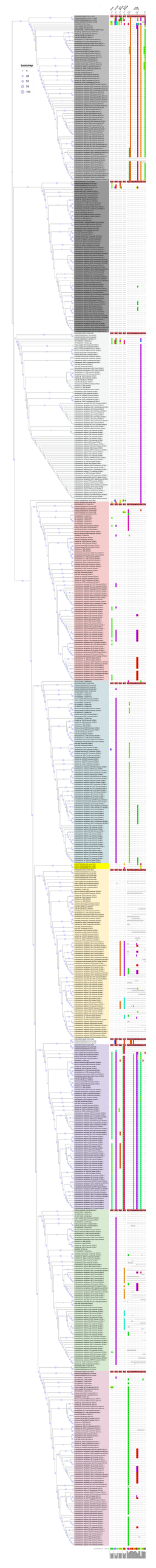
bootstrap
4
28
52
76
100

A

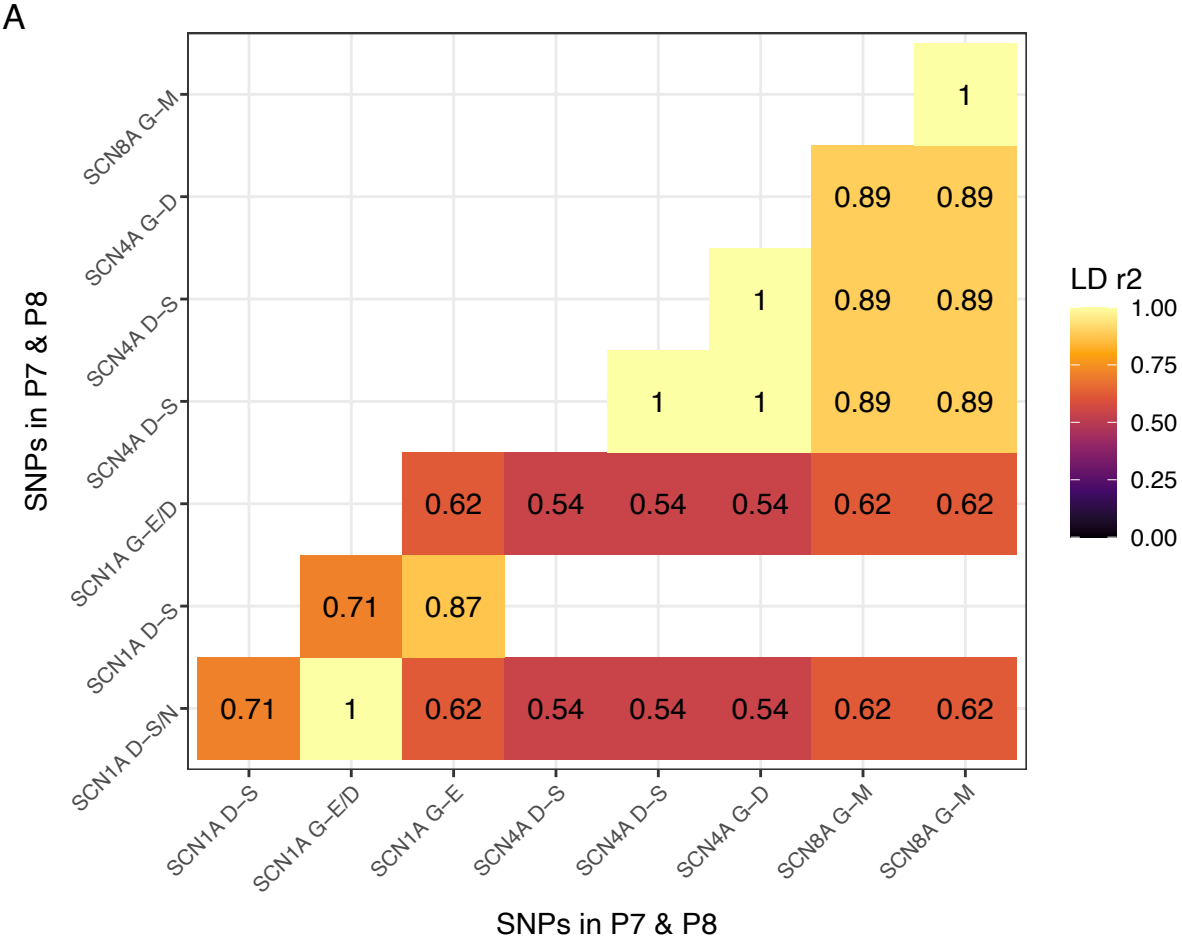
SNPs in P7 & P8
SCN8A G–M
SCN4A G–D
SCN4A D–S
SCN4A D–S
SCN1A G–E/D
SCN1A D–S
SCN1A D–S/N
1
0.89 0.89
1 0.89 0.89
1 1 0.89 0.89
0.62 0.54 0.54 0.54 0.62 0.62
0.71 0.87
0.71 1 0.62 0.54 0.54 0.54 0.62 0.62
SCN1A D–S
SCN1A G–E/D
SCN1A G–E
SCN4A D–S
SCN4A D–S
SCN4A G–D
SCN8A G–M
SCN8A G–M
SNPs in P7 & P8
LD r2
1.00
0.75
0.50
0.25
0.00

B

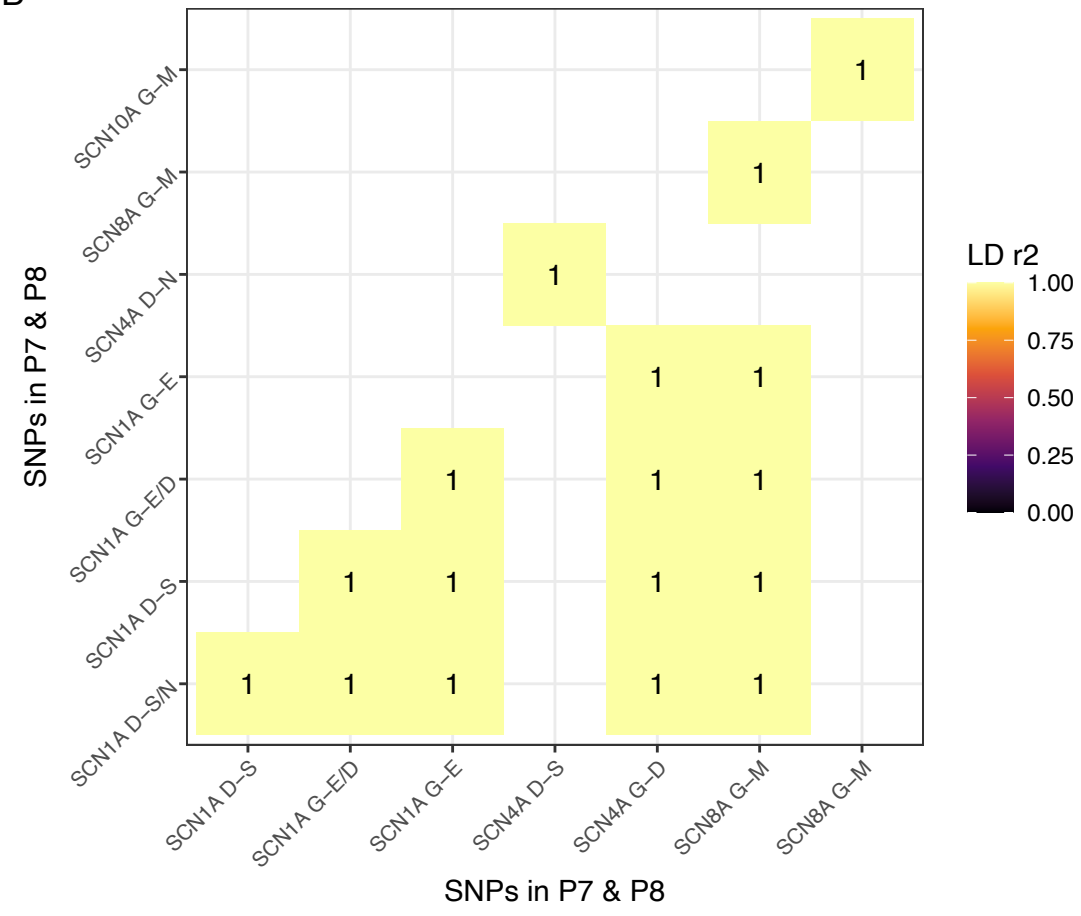
SNPs in P7 & P8
SCN10A G–M
SCN8A G–M
SCN4A D–N
SCN1A G–E
SCN1A G–E/D
SCN1A D–S
SCN1A D–S/N
1
1
1
1 1
1 1 1
1 1 1 1
1 1 1 1 1
SCN1A D–S
SCN1A G–E/D
SCN1A G–E
SCN4A D–S
SCN4A G–D
SCN8A G–M
SCN8A G–M
SNPs in P7 & P8
LD r2
1.00
0.75
0.50
0.25
0.00

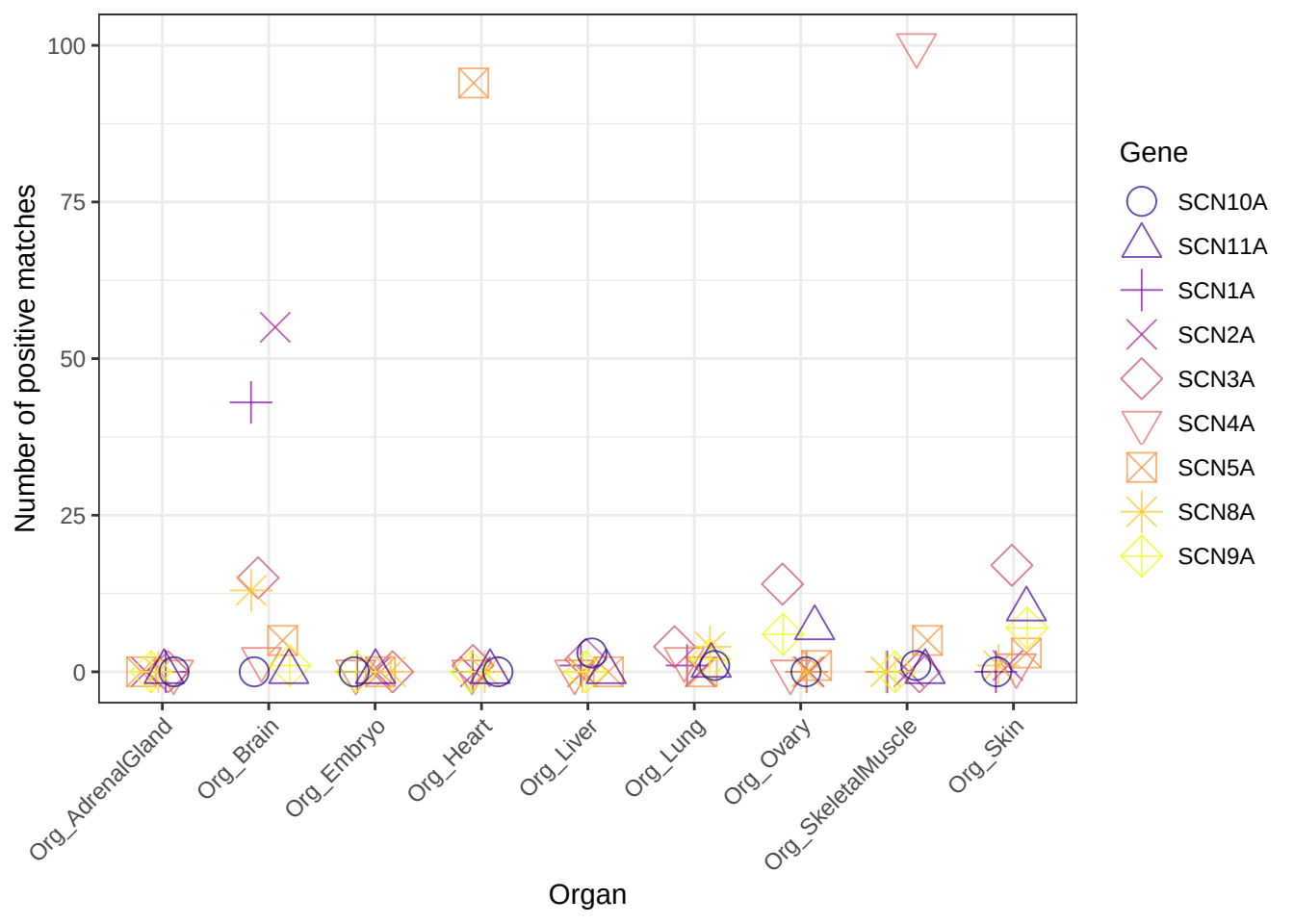
Number of positive matches
100
75
50
25
0
Org_AdrenalGland
Org_Brain
Org_Embryo
Org_Heart
Org_Liver
Org_Lung
Org_Ovary
Org_SkeletalMuscle
Org_Skin
Organ
Gene
SCN10A
SCN11A
SCN1A
SCN2A
SCN3A
SCN4A
SCN5A
SCN8A
SCN9A

Genus	species	Sample number	Tissue	Location	Latitude	Longitude	Loan from the Instituto de Ciencias Naturales ICN	Collection date	Collected by	Toxic prey reported for the species	Reported by	Sequence name	Total number of reads	Total of mapped reads	Samtools depth for the VGSC family	SRA accession number
Erythrolamprus	*epinephelus*	2052	Swab	El Cairo, Valle del Cauca	4.761248	-76.225751	No	January 2013	Fernando Vargas	*Phyllobates terriblis, Oophaga pumilio y Atelopus sp.*	Myers et al., 1978; Saporito et al., 2007; Feldman et al., 2012	Erythrolamprus_epinephelus_2052_ValledelCauca_	1256588	776051	38.27	SRR27351665
Erythrolamprus	*typhlus*	2138	Muscle	Tanimboca, Leticia, Amazonas	-4.127576	-69.953655	No	June 2013	Camilo Rodríguez	NA	NA	Erythrolamprus_typhlus_2138_Amazonas_	1811940	1138727	45.38	SRR27351686
Erythrolamprus	*reginae*	2160	Liver	San José del Guaviare, Guaviare	2.579343	-72.701531	No	4 January 2013	Martha Calderón	*Ameerega trivittata y Allobates sp.*	Martins & Oliveira, 1999; Pašukonis & Loretto, 2020	Erythrolamprus_reginae_2160_Guaviare_	1687730	1007857	46.46	SRR27351672
Xenopholis	sp.	2324	Swab	Tanimboca, Leticia, Amazonas	-4.127576	-69.953655	No	2014		*Allobates femoralis*	Ringler et al., 2010	Xenopholis_sp._2324_Amazonas_	1836124	1231851	66.73	SRR27351669
Oxybelis	sp.	2329	Tail	Tanimboca, Leticia, Amazonas	-4.127576	-69.953655	No	2014		NA	NA	Oxybelis_sp._2329_Amazonas_	2248838	2079244	94.04	SRR27351680
Erythrolamprus	*reginae*	2335	Muscle	Tanimboca, Leticia, Amazonas	-4.127576	-69.953655	No	2014		*Ameerega trivittata y Allobates sp.*	Martins & Oliveira, 1999; Pašukonis & Loretto, 2021	Erythrolamprus_reginae_2335_Amazonas_	2925784	1886358	83.85	SRR27351671
Erythrolamprus	*melanotus*	2527	Swab	Vereda Las Brisas, Puerto Salgar, Cundinamarca	5.495372	-74.645447	No	July 2014	Javier Mendéz	*Dendrobates truncatus*	NA	Erythrolamprus_melanotus_2527_Cundinamarca_	3194044	1918246	66.77	SRR27351677
Erythrolamprus	*melanotus*	2619	Tail	Vereda Las Brisas, Puerto Salgar, Cundinamarca	5.495372	-74.645447	No	July 2014	Javier Mendéz	*Dendrobates truncatus*	NA	Erythrolamprus_melanotus_2619_Cundinamarca_	1358548	754555	35.6	SRR27351676
Erythrolamprus	*epinephelus*	2627	Muscle	Pandi, Cundinamarca	4.193432	-74.485421	No	September 2014	Diego Goméz	*Phyllobates terriblis, Oophaga pumilio y Atelopus sp.*	Myers et al., 1978; Saporito et al., 2007; Feldman et al., 2013	Erythrolamprus_epinephelus_2627_Cundinamarca_	1403810	800360	59	SRR27351664
Xenodon	sp.	2635	Muscle	El Nilo, Cundinamarca	4.306568	-74.631007	No	November 2014	Sebastián di Domenico	NA	NA	Xenodon_sp._2635_Cundinamarca_	886950	586506	32.2	SRR27351679
Erythrolamprus	*epinephelus*	2637	Tail	Salero, Chocó	5.358701	-76.646274	No	November, 2014	Jonar David Echavarria	*Phyllobates terriblis, Oophaga pumilio y Atelopus sp.*	Myers et al., 1978; Saporito et al., 2007; Feldman et al., 2014	Erythrolamprus_epinephelus_2637_Choco_	781256	503536	40.37	SRR27351663
Leptodeira	sp.	2654	Muscle	El Nilo, Cundinamarca	4.306568	-74.631007	No	November 2014	Sebastián di Domenico	*Bufonidae y Leptodactylus* sp.	Moore et al., 2009	Leptodeira_sp._2654_Cundinamarca_	1087086	768121	38.26	SRR27351682
Indet		2667	Muscle	Tanimboca, Leticia, Amazonas	-4.127576	-69.953655	No	19 April 2015	Camilo Rodríguez	NA	NA	Indet_2667_Amazonas_	981758	653147	40.08	SRR27351684
Imantodes	*cenchoa*	2671	Muscle	Tanimboca, Leticia, Amazonas	-4.127576	-69.953655	No	19 April 2015	Camilo Rodríguez	NA	NA	Imantodes_cenchoa_2671_Amazonas_	1474608	302982	42.38	SRR27351685
Anillius	*scytale*	2673	Muscle	Tanimboca, Leticia, Amazonas	-4.127576	-69.953655	No	19 April 2015	Camilo Rodríguez	NA	NA	Anilius_scytale2_2673_Amazonas_	1534248	938718	50.99	SRR27351694
Micrurus	*hemprichii*	2683	Muscle	Tanimboca, Leticia, Amazonas	-4.127576	-69.953655	No	December 2015	Camilo Rodríguez	Elapid snake	NA	Micrurus_hemprichii_2683_Amazonas_	253494	105081	29.56	SRR27351681
Erythrolamprus	*epinephelus*	2715	Muscle	Salero, Chocó	5.358701	-76.646274	No	February, 2015	Jonar David Echavarria	*Phyllobates terriblis, Oophaga pumilio y Atelopus sp.*	Myers et al., 1978; Saporito et al., 2007; Feldman et al., 2015	Erythrolamprus_epinephelus_2715_Choco_	1974580	1099925	40.16	SRR27351692
Erythrolamprus	*reginae*	2725	Muscle	Tanimboca, Leticia, Amazonas	-4.127576	-69.953655	No	19 April 2015	Camilo Rodríguez	*Ameerega trivittata y Allobates sp.*	Martins & Oliveira, 1999; Pašukonis & Loretto, 2021	Erythrolamprus_reginae_2725_Amazonas_	929410	571811	31.71	SRR27351662
Erythrolamprus	*reginae*	2726	Muscle	Tanimboca, Leticia, Amazonas	-4.127576	-69.953655	No	19 April 2015	Camilo Rodríguez	*Ameerega trivittata y Allobates sp.*	Martins & Oliveira, 1999; Pašukonis & Loretto, 2022	Erythrolamprus_reginae_2726_Amazonas_	1549044	984442	71.67	SRR27351661
Erythrolamprus	*reginae*	2727	Muscle	Tanimboca, Leticia, Amazonas	-4.127576	-69.953655	No	19 April 2015	Camilo Rodríguez	*Ameerega trivittata y Allobates sp.*	Martins & Oliveira, 1999; Pašukonis & Loretto, 2023	Erythrolamprus_reginae_2727_Amazonas_	889910	554819	49.64	SRR27351660
Dendrophidion	sp.	2728	Muscle	Tanimboca, Leticia, Amazonas	-4.127576	-69.953655	No	19 April 2015	Camilo Rodríguez	Leptodactylidae	da Costa et al., 2007	Dendrophidion_sp._2728_Amazonas_	2626194	2312102	47.41	SRR27351667
Erythrolamprus	*reginae*	2734	Tail	Tanimboca, Leticia, Amazonas	-4.127576	-69.953655	No	23 February 2015	Camilo Rodríguez	*Ameerega trivittata y Allobates sp.*	Martins & Oliveira, 1999; Pašukonis & Loretto, 2024	Erythrolamprus_reginae_2734_Amazonas_	871918	540503	41.72	SRR27351659
Erythrolamprus	*epinephelus*	2743	Muscle	Samurindó, Chocó	5.586063	-76.65271	No	16 June 2015	Pablo Palacios	*Phyllobates terriblis, Oophaga pumilio y Atelopus sp.*	Myers et al., 1978; Saporito et al., 2007; Feldman et al., 2016	Erythrolamprus_epinephelus_2743_Choco_	1407946	780031	34.05	SRR27351691

Genus	species	Sample number	Tissue	Location	Latitude	Longitude	Loan from the Instituto de Ciencias Naturales ICN	Collection date	Collected by	Toxic prey reported for the species	Reported by	Sequence name	Total number of reads	Total of mapped reads	Samtools depth for the VGSC family	SRA accession number
Erythrolamprus	*epinephelus*	2818	Tail	Armenia, Quindío	4.514719	-75.728273	No	9 September 2015	Fernando Vargas	*Phyllobates terriblis, Oophaga pumilio y Atelopus sp.*	Myers et al., 1978; Saporito et al., 2007; Feldman et al., 2017	Erythrolamprus_epinephelus_2818_Quindio_	2415800	1297113	31.13	SRR27351690
Erythrolamprus	*epinephelus*	2819	Tail	Armenia, Quindío	4.514719	-75.728273	No	9 September 2015	Fernando Vargas	*Phyllobates terriblis, Oophaga pumilio y Atelopus sp.*	Myers et al., 1978; Saporito et al., 2007; Feldman et al., 2018	Erythrolamprus_epinephelus_2819_Quindio_	2031030	1260041	56.41	SRR27351689
Dendrophidion	*percarinatum*	2820	Swab	Victoria, Chocó	5.510271	-76.870179	No	12 November 2015	Pablo Palacios	NA	NA	Dendrophidion_percarinatum_2820_Choco_	1620156	1447769	47.66	SRR27351668
Erythrolamprus	*reginae*	2823	Tail	Santa María, Boyacá	4.883333	-73.25	No	1 November 2015	Sebastián di Domenico	*Ameerega trivittata y Allobates sp.*	Martins & Oliveira, 1999; Pašukonis & Loretto, 2021	Erythrolamprus_reginae_2823_Boyaca_	1762468	929956	39.76	SRR27351658
Erythrolamprus	*melanotus*	2824	Tail	Puerto Boyacá, Boyacá	5.967765	-74.594422	No	1 November 2015	Alvaro	*Dendrobates truncatus*	NA	Erythrolamprus_melanotus_2824_Boyaca_	1151054	696894	36.84	SRR27351675
Bothrops	*atrox*	2841	Muscle	Bojonawi, Vichada	4.422513	-69.293534	No	5 December 2015		Viperid snake	NA	Bothrops_atrox2_2841_Vichada_	1191006	770283	14.85	SRR27351693
Chironius	sp.	3005	Liver	Unknown	NA	NA	No	March 2015	Carlos Eduardo Burbano	NA	NA	Chironius_sp._3005_	1260596	1148728	72.65	SRR27351655
Erythrolamprus	*melanotus*	GDD1066	Liver	Caucasia, Antioquia	7.983238	-75.216681	Yes	Unknown		NA	NA	Erythrolamprus_melanotus_GDD1066_Antioquia_	1298420	834553	40.33	SRR27351678
Erythrolamprus	*sp.*	GDD149	Liver	Salamina, Caldas	5.414167	-75.49086	Yes	Unknown		NA	NA	Erythrolamprus_sp._GDD149_Caldas_	1952682	1233236	101.58	SRR27351656
Erythrolamprus	*epinephelus*	GDD780	Liver	Salamina, Caldas	5.414167	-75.49086	Yes	Unknown		*Phyllobates terriblis, Oophaga pumilio y Atelopus sp.*	Myers et al., 1978; Saporito et al., 2007; Feldman et al., 2019	E. epinephelus_pseudocobella_GDD780_Caldas_	2934160	1757575	136.44	SRR27351688
Xenodon	sp.	MAA563	Liver	Orocue, Casanare	4.910406	-71.434187	Yes	Unknown		NA	NA	Xenodon_sp._MAA563_Casanare_	1651884	1040052	76.74	SRR27351670
Erythrolamprus	*aesculapii*	MLC1078	Liver	San José del Guaviare, Guaviare	2.579343	-72.701531	Yes	Unknown	Martha Calderón	NA	NA	Erythrolamprus_aesculapii_MLC1078_Guaviare_	1341098	718798	33.12	SRR27351666
Erythrolamprus	*epinephelus*	MLC1233	Liver	Tumaco, Nariño	1.59251	-78.71841	Yes	Unknown	Martha Calderón	*Phyllobates terriblis, Oophaga pumilio y Atelopus sp.*	Myers et al., 1978; Saporito et al., 2007; Feldman et al., 2020	Erythrolamprus_epinephelus_MLC1233_Narino_	839978	556962	37.72	SRR27351687
Indet		MLC384	Liver	Puerto Boyacá, Boyacá	5.967765	-74.594422	Yes	Unknown	Martha Calderón	NA	NA	Indet_MLC384_Boyaca_	1741704	1591697	52.09	SRR27351683
Erythrolamprus	*reginae*	MLC943	Liver	San José del Guaviare, Guaviare	2.579343	-72.701531	Yes	Unknown	Martha Calderón	*Ameerega trivittata y Allobates sp.*	Martins & Oliveira, 1999; Pašukonis & Loretto, 2021	Erythrolamprus_reginae_MLC943_Guaviare_	1529356	961647	60.52	SRR27351657
Chironius	*fuscus*	NON16	Liver	Cordoba	8.315783	-75.763029	Yes	Unknown		*Dendrobates* sp.	Martins & Oliveira, 1999	Chironius_fuscus_NON16_Cordoba_	819994	761840	31.49	SRR27351674
Erythrolamprus	*melanotus*	ORP074	Liver	Cordoba	8.315783	-75.763029	Yes	Unknown		*Dendrobates truncatus*	NA	Erythrolamprus_melanotus_ORP074_Cordoba_	2767184	1753635	53.87	SRR27351673
												Mean	1582009.45	1026393.8	51.2375	
												SD	668034.3888	498224.9183	23.02558908	

Family name	Protein	Gene	Organism used for design	Target sequence length (bp)	Genbank number
Voltage-gated sodium channel (alpha subunit)	NaV1.1	SCN1A	*Thamnophis sirtalis*	5542	BK008860.1
	NaV1.2	SCN2A	*Thamnophis sirtalis*	5747	BK008861.1
	NaV1.3	SCN3A	*Thamnophis sirtalis*	6012	BK008862.1
	NaV1.4	SCN4A	*Thamnophis sirtalis*	5628	BK008863.1
	NaV1.5	SCN5A	*Python bivittatus*	2706	AEQU02000001.1
	NaV1.6	SCN8A	*Thamnophis sirtalis*	5964	BK008864.1
	NaV1.7	SCN9A	*Thamnophis sirtalis*	5895	BK008865.1
	NaV1.8	SCN10A	*Python bivittatus*	1883	AEQU02000001.1
	NaV1.9	SCN11A	*Python bivittatus*	2003	AEQU02000001.1
Nicotinic receptor	Alpha1	CHRNA1	*Ophiophagus hannah*	1530	PRJNA201683
	Alpha2	CHRNA2	*Python bivittatus*	1545	AEQU02000001.1
	Alpha3	CHRNA3	*Python bivittatus*	1899	AEQU02000001.1
	Alpha4	CHRNA4	*Python bivittatus*	1272	AEQU02000001.1
	Alpha5	CHRNA5	*Python bivittatus*	1485	AEQU02000001.1
	Alpha6	CHRNA6	*Python bivittatus*	1188	AEQU02000001.1
	Alpha7	CHRNA7	*Ophiophagus hannah*	1464	PRJNA201683
	Alpha9	CHRNA9	*Python bivittatus*	1524	AEQU02000001.1
	Alpha10	CHRNA10	*Python bivittatus*	1089	AEQU02000001.1
	Beta1	CHRNB1	*Ophiophagus hannah*	1518	PRJNA201683
	Beta2	CHRNB2	*Python bivittatus*	1374	AEQU02000001.1
	Beta3	CHRNB3	*Python bivittatus*	1383	AEQU02000001.1
	Beta4	CHRNB4	*Python bivittatus*	1566	AEQU02000001.1
	Delta	CHRND	*Python bivittatus*	1608	AEQU02000001.1
	Epsilon	CHRNE	*Python bivittatus*	1619	AEQU02000001.1
	Gamma	CHRNG	*Python bivittatus*	2313	AEQU02000001.1
Canal de calcio voltaje dependiente (Subunidad alfa)	CaV1.1	CACNA1S	*Ophiophagus hannah*	2808	PRJNA201683
	Cav1.2	CACNA1C	*Python bivittatus*	1239	AEQU02000001.1
	CaV1.3	CACNA1D	*Python bivittatus*	5715	AEQU02000001.1
	CaV1.4	CACNA1F	*Python bivittatus*	6375	AEQU02000001.1
	CaV2.1	CACNA1A	*Python bivittatus*	6909	AEQU02000001.1
	CaV2.2	CACNA1B	*Python bivittatus*	1574	AEQU02000001.1
	CaV2.3	CACNA1E	*Python bivittatus*	6870	AEQU02000001.1
	CaV3.1	CACNA1G	*Python bivittatus*	5931	AEQU02000001.1
	CaV3.2	CACNA1H	*Python bivittatus*	3855	AEQU02000001.1
	CaV3.3	CACNA1I	*Python bivittatus*	6510	AEQU02000001.1
Voltage-gated calcium channel (alpha subunit)	Kv1.1	KCNA1	*Python bivittatus*	1485	AEQU02000001.1
	Kv1.2	KCNA2	*Python bivittatus*	1500	AEQU02000001.1
	Kv1.3	KCNA3	*Ophiophagus hannah*	1467	PRJNA201683
	Kv1.4	KCNA4	*Ophiophagus hannah*	1347	PRJNA201683
	Kv1.5	KCNA5	*Python bivittatus*	1683	PRJNA201683
	Kv1.7	KCNA7	*Ophiophagus hannah*	1542	PRJNA201683
	Kv1.8	KCNA10	*Ophiophagus hannah*	2016	PRJNA201683
Voltage-gated	Kv2.1	KCNB1	*Ophiophagus hannah*	588	PRJNA201683
	Kv2.2	KCNB2	*Python bivittatus*	2724	AEQU02000001.1
	Kv3.1	KCNC1	*Python bivittatus*	1863	AEQU02000001.1

potassium channel (Shaw - subfamily C)	Kv3.2	KCNC2	*Python bivittatus*	1137	AEQU02000001.1
	Kv3.4	KCNC4	*Python bivittatus*	1884	AEQU02000001.1
Voltage-gated potassium channel (Shal - subfamily D)	Kv4.1	KCND1	*Python bivittatus*	1706	AEQU02000001.1
	Kv4.2	KCND2	*Python bivittatus*	1896	AEQU02000001.1
	Kv4.3	KCND3	*Ophiophagus hannah*	1110	PRJNA201683
Voltage-gated potassium channel (subfamily F)	Kv5.1	KCNF1	*Python bivittatus*	702	AEQU02000001.1
Voltage-gated potassium channel (subfamily G)	Kv6.1	KCNG1	*Ophiophagus hannah*	1464	PRJNA201683
	Kv6.2	KCNG2	*Python bivittatus*	1533	AEQU02000001.1
	Kv6.3	KCNG3	*Ophiophagus hannah*	1575	PRJNA201683
	Kv6.4	KCNG4	*Python bivittatus*	1332	AEQU02000001.1
Voltage-gated potassium channel (eag - subfamily H)	Kv10.1	KCNH1	*Python bivittatus*	1527	AEQU02000001.1
	Kv11.1	KCNH2	*Python bivittatus*	987	AEQU02000001.1
	Kv12.2	KCNH3	*Python bivittatus*	1737	AEQU02000001.1
	Kv12.3	KCNH4	*Python bivittatus*	2880	AEQU02000001.1
	Kv10.2	KCNH5	*Python bivittatus*	3126	AEQU02000001.1
	Kv11.2	KCNH6	*Python bivittatus*	2943	AEQU02000001.1
	Kv11.3	KCNH7	*Python bivittatus*	3168	AEQU02000001.1
	Kv12.1	KCNH8	*Python bivittatus*	3510	AEQU02000001.1
Voltage-gated potassium channel (KGT subfamily Q)	Kv7.1	KCNQ1	*Python bivittatus*	3324	AEQU02000001.1
	Kv7.2	KCNQ2	*Python bivittatus*	1977	AEQU02000001.1
	Kv7.3	KCNQ3	*Python bivittatus*	1228	AEQU02000001.1
	Kv7.4	KCNQ4	*Python bivittatus*	2121	AEQU02000001.1
	Kv7.5	KCNQ5	*Python bivittatus*	1893	AEQU02000001.1
Voltage-gated potassium channel (subfamily S)	Kv9.1	KCNS1	*Python bivittatus*	2652	AEQU02000001.1
	Kv9.2	KCNS2	*Python bivittatus*	1401	AEQU02000001.1
	Kv9.3	KCNS3	*Python bivittatus*	1434	AEQU02000001.1
Voltage-gated potassium channel (subfamily V)	Kv8.1	KCNV1	*Python bivittatus*	1512	AEQU02000001.1
	Kv8.2	KCNV2	*Python bivittatus*	1275	AEQU02000001.1
Recombination activating gene 1	RAG-1	RAG1	*Thamnophis sirtalis*	1578	XM_014075888.1
Proto-oncogen	c-mos	MOS	*Erythrolamprus reginae*	600	GQ895819.1
Na+/K+ pump Sodium-potassium ATPase pump	ATP1A1	ATP1A1	*Protobothrops mucrosquamatus*	3560	XM_015818080.2
Total	76 genes			188530	

Ensembl gene ID	**Gene ID**	**Gene name**	**Gene name in P. guttatus genome**	**Region name in *P. guttatus* genome**	**Scaffold in *P. guttatus* genome**	**Start position**	**End position**	**Strand**	**Blast exons sequence organism**	**Number of exons**	***T. sirtalis* GenBank ID**	***P. guttatus* genome exons location**	**Final number of exons obtained in consensus sequences**
ENSG00000185313	6336	SCN10A	SCN10A	LOC117654779	NW_023010900.1	4655826	4745976	positive	*Pantherophis guttatus*	Unknown	NA	>NW_023010900.1:4745742-4745976 >NW_023010900.1:4733142-4733270 >NW_023010900.1:4732282-4732393 >NW_023010900.1:4729093-4729222 >NW_023010900.1:4723382-4723474 >NW_023010900.1:4721962-4722172 >NW_023010900.1:4720944-4721008 >NW_023010900.1:4717495-4717637 >NW_023010900.1:4705653-4705851 >NW_023010900.1:4704506-4704662 >NW_023010900.1:4701801-4702200 >NW_023010900.1:4697639-4697766 >NW_023010900.1:4696160-4696399 >NW_023010900.1:4693380-4693593 >NW_023010900.1:4692383-4692737 >NW_023010900.1:4691710-4692130 >NW_023010900.1:4690255-4690375 >NW_023010900.1:4683255-4683379 >NW_023010900.1:4680302-4680457 >NW_023010900.1:4677148-4677322 >NW_023010900.1:4675396-4675519 >NW_023010900.1:4663461-4663601 >NW_023010900.1:4662734-4662840 >NW_023010900.1:4660239-4660510 >NW_023010900.1:4655825-4658206	1 (only NW_023010900.1:4655825-4658206)
ENSG00000168356	11280	SCN11A	SCN11A	LOC117654780	NW_023010900.1	4780111	4814439	positive	*Pantherophis guttatus*	Unknown	NA	>NW_023010900.1:4814022-4814439 >NW_023010900.1:4810452-4810866 >NW_023010900.1:4807935-4808046 >NW_023010900.1:4804784-4804893 >NW_023010900.1:4801088-4801243 >NW_023010900.1:4800193-4800367 >NW_023010900.1:4797970-4798099 >NW_023010900.1:4796334-4796544 >NW_023010900.1:4794216-4794273 >NW_023010900.1:4791630-4791772 >NW_023010900.1:4790079-4790180 >NW_023010900.1:4784648-4784919 >NW_023010900.1:4780110-4781267	1 (only NW_023010900.1:4780110-4781267)
ENSG00000183873	6331	SCN5A	LOC117654807	LOC117654807	NW_023010900.1	4267418	4641777	positive	*Pantherophis guttatus*	Unknown	NA	Artificial exons created by mapping *X. tropicalis* , *G. gallus* exons *againts P. guttatus* genome (ENSXETG00000004251, ENSGALG00000006112)	1 (only artificial exon 26 NW_023010900.1:4240810-4242090, see Supp fasta sequence PanGut_SCN5A_exon
ENSG00000007314	6329	SCN4A	SCN4A	LOC117664772	NW_023010717.1	15870385	16001819	positive	*Thamnophis sirtalis*	26 (10a-b)	KJ908920, KJ908899, KJ908873, KJ908907	NA. Domain 4 DG variant 15998696-701	26
ENSG00000153253	6328	SCN3A	LOC117670973	LOC117670973	NW_023010694.1	29423555	29504825	negative	*Thamnophis sirtalis*	26 (5a-b)	KJ908864, KJ908874, KJ908876, KJ908896, KJ908912, KJ908917	NA	26
ENSG00000136531	6326	SCN2A	SCN2A	LOC117670994	NW_023010694.1	29523345	29636194	positive	*Thamnophis sirtalis*	26 (5a-b)	KJ908862, KJ908876, KJ908914, KJ908934, KJ908936	NA	26

ENSG00000144285	6323	SCN1A	SCN1A	LOC117671051	NW_023010694.1	29853090	29956985	negative	*Thamnophis sirtalis*	26 (5a-b)	KJ908875, KJ908900, KJ908903, KJ908904, KJ908930	NA	26
ENSG00000169432	6335	SCN9A	SCN9A	LOC117671080	NW_023010694.1	29980741	30103981	negative	*Thamnophis sirtalis*	26 (5a-b)	KJ908861, KJ908865, KJ90879, KJ908889, KJ908913, KJ908918, KJ908929, KJ908931, KJ908932, KM066119	NA	26
ENSG00000196876	6334	SCN8A	SCN8A	SCN8A	NW_023010713.1	7660736	7777256	negative	*Thamnophis sirtalis*	26 (5a-b)	KJ908863, KJ908869, KJ908872, KJ908891, KJ908892, KJ908908, KJ908922, KJ908928, KJ908933, KJ908935, KJ908937	NA	26

Species	Common name	SCN1A	SCN2A	SCN3A	SCN4A	SCN5A	SCN7A	SCN8A	SCN9A	SCN10A	SCN11A	CACNA1A
Homo sapiens	Human	ENSG00000144285	ENSG00000136531	ENSG00000153253	ENSG00000007314	ENSG00000183873	ENSG00000136546	ENSG00000196876	ENSG00000169432	ENSG00000185313	ENSG00000168356	ENSG00000141837
Mus musculus	Mouse	ENSMUSG00000064329	ENSMUSG00000075318	ENSMUSG00000057182	ENSMUSG00000001027	ENSMUSG00000032511	ENSMUSG00000034810	ENSMUSG00000023033	ENSMUSG00000075316	ENSMUSG00000034533	ENSMUSG00000034115	ENSMUSG00000034656
Rattus norvegicus	*Brown rat*	ENSRNOG00000053122	ENSRNOG00000005018	ENSRNOG00000005007	ENSRNOG00000012134	ENSRNOG00000015049	ENSRNOG00000029342	ENSRNOG00000005309	ENSRNOG00000006639	ENSRNOG00000032473	ENSRNOG00000032884	ENSRNOG00000052707
Pelodiscus sinensis	Chineese softshell turtle	NA	XP_006137387.1	ENSPSIG00000002683	ENSPSIG00000007410		NA	ENSPSIG00000016907	NA	NA	NA	NA
Xenopus (Silurana) tropicalis	Tropical clawed frog	ENSXETG00000020846	ENSXETG00000021004	ENSXETG00000008965	ENSXETG00000014235	ENSXETG00000004251	NA	XP_031751845.1	NA	NA	NA	ENSXETG00000005585
Gallus gallus	Chicken	NA	ENSGALG00000011009	ENSGALG00000011040	ENSGALG00000034427	ENSGALG00000006112	NA	ENSGALG00000043728	ENSGALG00000027793	NA	ENSGALG00000027702	NA
Anolis carolinensis	Green anole	XP_016850756.1	XP_008113359.1	ENSACAG00000001038	ENSACAG00000012739	XP_016853093.1	NA	XP_003216967.1	NA	ENSACAG00000009381	DAA34938.1	XP_016851635.1
Crocodylus porosus	Australian saltwater crocodile	XP_019409121.1	NA	NA	NA	NA	NA	NA	NA	NA	NA	NA
Crotalus tigris	Tiger rattlesnake	NA	XP_039208732.1	NA	NA	NA	NA	XP_039225747.1	NA	NA	NA	XP_039198770.1
Gekko japonicus		XP_015271637.1	NA	NA	XP_015273726.1	NA	NA	NA	NA	NA	NA	XP_015274358.1
Lacerta agilis		NA	NA	NA	NA	XP_033020790.1	NA	NA	NA	NA	NA	XP_032995621.1
Notechis scutatus	mainland tiger snake	NA	NA	NA	NA	NA	NA	XP_026537110.1	NA	NA	NA	NA
Pantherophis guttatus		NA	XP_034282445.1	NA	NA	NA	NA	XP_034268352.1	NA	NA	NA	XP_034262813.1
Podarcis muralis	Common wall lizard	NA	XP_028603348.1	NA	XP_028558585.1	NA	NA	XP_028566865.1	NA	NA	NA	XP_028573171.1
Pogona vitticeps	central bearded dragon	XP_020645073.1	NA	NA	XP_020653693.1	NA	NA	NA	NA	NA	NA	XP_020656028.1
Protobothrops mucrosquamatus		XP_015679123.1	NA	NA	NA	NA	NA	NA	NA	NA	NA	XP_029139859.1
Pseudonaja textilis		NA	XP_026552908.1	NA	NA	NA	NA	NA	NA	NA	NA	XP_026551939.1
Python bivittatus	Burmese python	XP_025024892.1	NA	NA	XP_025020302.1	NA	NA	NA	NA	XM_025170661.1	NA	XP_025024299.1
Thamnophis elegans	Western terrestrial garter snake	NA	XP_032088260.1	NA	NA	NA	NA	XP_032066422.1	NA	NA	NA	XP_032094925.1
Thamnophis sirtalis	Garter snake	DAA64620.1	BK008861	DAA64622.1	AAW68223.1	NA	NA	XP_013919059.1	DAA64625.1	NA	NA	XP_013919992.1
Zootoca vivipara	common lizard	NA	NA	NA	XP_034990651.1	NA	NA	XP_034959711.1	NA	NA	NA	XP_034960755.1

Gene	Statistic	*E. melanotus* populations	*E. epinephelus* populations	*E. reginae* populations
SCN4A	pi	0.00110134	0.00623501	0.00481437
SCN4A	segre_sites	4	27	18
SCN4A	parsi_sites	3	18	16
SCN4A	TajiD	-0.0982008	0.0969218	0.429003
SCN4A	P_tajiD	0.51931	0.451365	0.337249
SCN1A	pi	0.00381741	0.00851769	0.0147774
SCN1A	segre_sites	7	21	36
SCN1A	parsi_sites	4	18	21
SCN1A	TajiD	0.0615766	-0.168225	-0.403858
SCN1A	P_tajiD	0.460798	0.548656	0.632769
SCN8A	pi	0.00103455	0.00684603	0.00578833
SCN8A	segre_sites	4	21	31
SCN8A	parsi_sites	2	21	16
SCN8A	TajiD	-0.82229	0.924114	-1.3866
SCN8A	P_tajiD	0.76534	0.189834	0.916945
SCN5A	pi	0.0013435	0.00644039	0.00661084
SCN5A	segre_sites	4	33	25
SCN5A	parsi_sites	3	20	22
SCN5A	TajiD	0.625888	-0.658467	0.302653
SCN5A	P_tajiD	0.281088	0.723216	0.379728
SCN9A	pi	0.00097629	0.0064706	0.00299235
SCN9A	segre_sites	7	22	14
SCN9A	parsi_sites	0	19	13
SCN9A	TajiD	-1.83913	1.8508	0.0745492
SCN9A	P_tajiD	0.985512	0.0362667	0.46006
SCN10A	pi	0.00284818	0.0114683	0.010454
SCN10A	segre_sites	8	53	36
SCN10A	parsi_sites	5	37	31
SCN10A	TajiD	0.146031	-0.750273	-0.096777
SCN10A	P_tajiD	0.433441	0.753235	0.520843
SCN11A	pi	0.00456442	0.0149666	0.0101428
SCN11A	segre_sites	17	58	29
SCN11A	parsi_sites	2	37	25
SCN11A	TajiD	-1.64072	-1.09902	-0.046264
SCN11A	P_tajiD	0.961922	0.853184	0.503815

Region	Position in this study	Gene	Amino acid change	Presence in samples from this study	Organisms with substitutions at this site	Reference
DII S1	NA	SCN4A	N1025N	All snakes	All snakes, mice, change to D in birds. N in Pith	Bodawatta et al., 2022
DII S5	In Fig 2 position 2	SCN4A	S719N	In *E. reginae* and *E. aesculapii*	*Thamnophis spp.* and *Heterodon platirhinos*	Genbank ref: FJ570810, FJ570811, FJ570812, BK008863 and KT277703
DI p-loop	In Fig 2 position 1	SCN4A	I419L	In E. reginae and E. aesculapii	Dendrobatidae frogs	Genbank ref: KT989187
		SCN9A	I380L	E. reginae, E. sp, E. epinephelus, E. typhlus	Dendrobatidae frogs in SCN4A	NA for this ortholog
	NA	SCN8A	F371Y	Fixed in *E. epinephelus*	Tetrodotoxic newts	Vaelli et al. 2020; Gendreau et al., 2021
	NA	SCN4A	V748I	*Bothrops atrox* , *E* . sp and *Xenopholis* sp.	Dendrobatidae frogs	Márquez et al., 2018
DIII p-loop	In Fig 2 position 4*	SCN2A[a–b]	D1427G/Y	*E. epinephelus, E. reginae*	In SCN4A in *A. pryeri* and *T. atractus*	Feldman et al. 2012; McGlothin et al. 2016
		SCN3A[a]	D1373N/Y	Fixed in E. epinephelus and E. reginae. Present in *E* . sp		
		SCN9A	D1408E	Present in all snakes		
DIV p-loop	In Fig 2 position 5	SCN1A[a]	Q1719M	Present in all snakes and A. carolinensis	*T. granulosa*	Vaeilli et al. 2020
		SCN2A[a–b]	Q1710M	E. reginae, E. epinephelus and Imantodes cenchoa	In SCN1A and SCN3A in *T. granulosa*	
		SCN3A[a]	Q1656M/L	*E. reginae* and *E.* sp	*T. granulosa*	
	In Fig 2 position 6**	SCN8A	I1699V	*Erythrolamprus, Leptodeira, Imantodes, Xenopholis* and *Micrurus*	Present in several colubrid genera. *T. granulosa* (SCN4A and SCN8A)	McGlothin et al. 2016; Perry et al., 2018; Gendreau et al., 2021
		SCN11A	I1526M/V	Fixed in *E. epinephelus. Chironius fuscus* and *Chironius* sp.	*T. sirtalis*	
	In Fig 2 position 7***	SCN1A[a]	D1727S/N	*E. epinephelus, E. sp* and *E. reginae*	In TTX resistant organism in other orthologs	None for SCN1A, SCN2A and SCN3A orthologs. For SCN4A Josh et al. 2008; Feldman et al. 2012; Hanifin & Gilly, 2015
		SCN2A[a–b]	D1718N	E. epinephelus		
		SCN3A[a]	D1664N/S	*E. epinephelus* and *E* . sp		
		SCN4A	D1533S/N	*E. epinephelus, E* . sp. and *E. reginae*	In pufferfish, tetrodotoxic newts, and *Thamnophis snakes*	
		SCN9A	D1699N	Present in all snakes	Across all snakes	McGlothin et al. 2016
		SCN11A	D1533N	*Anilius scytale*	*T. sirtalis*	Perry et al., 2018
	In Fig 2 position 8***	SCN1A[a]	G1728S/E	*E. epinephelus, E. sp.* and *E. reginae*	Tetrodotoxic newts and pufferfish	Josh et al. 2008; Vaelli et al. 2020; Gendreau et al. 2021
		SCN2A[a–b]	G1719D	E. epinephelus	*Tetrodotoxic newts*	Vaelli et al. 2020; Gendreau et al. 2021
		SCN3A[a]	G1665D/V/E	*E. epinephelus, E* . sp. and *E. reginae*	In TTX resistant organism in other orthologs	NA for this ortholog
		SCN4A	G1533D	*E. epinephelus, E* . sp. and *E. reginae*	In pufferfish, tetrodotoxic newts, and *Thamnophis snakes*	Josh et al. 2008; Feldman et al. 2012; Hanifin & Gilly, 2015
		SCN8A	G1707M	*E. epinephelus, E* . sp. and *E. reginae*	In *E. epinephelus*	McGlothin et al. 2016
		SCN9A	G1700Y/S/A	Present in all snakes	Across reptiles	McGlothin et al. 2014; McGlothin et al. 2016; Perry et al. 2018
		SCN10A	G1666M	*E. reginae*		
		SCN11A	A1534E	Present in all snakes		
	In Fig 2 position 9	SCN2A[a–b]	P1729R	*E. epinephelus, E. reginae, E. melanotus* and *E. typhlus*	Dendrobatidae frogs in SCN4A	NA for this ortholog
		SCN3A[a]	P1675R	*E. melanotus* and *E.* sp.		
		SCN4A	P1544S	*E. reginae* and *E. epinephelus*	Dendrobatidae frogs	KT989154, KT989158
DI S6	NA	SCN11A	I394V****	Present in several snakes genera. Including *Erythrolamprus*	Dendrobatidae frogs in SCN4A	Tarvin et al. 2016; Márquez et al., 2018
	A443D-SCN4A	SCN11A	E406D	Present in all snakes	Mantella and Dendrobatie frogs in SCN4A	Tarvin et al. 2016; Márquez et al., 2018
	E406D-SCN11A	SCN4A	A443D	*Erythrolamprus* genus		

DII S6	NA	SCN4A	T774L/V	Leptodeira, *Dendriphidion, Oxybelis, Chironius* and *E. epinephelus*	Dendrobatidae frogs	Márquez et al., 2018

[a]Amphibian's SCN1A, SCN2A, and SCN3A are not orthologs for SCN1A, SCN2A and SCN3A in mammals and reptiles.

[b]SCN2A is paraphyletic between reptiles and mammals. Amino acid notations are based on the Mus musculus SCN2A, however, this is not a reptile SCN2A orth

*Reported as a TTX and STX target site from structural models (Terlau et al. 1991)

**Site reported to confer moderate TTX resistance (Geffeney et al. 2005; Vaelli et al. 2016)

***Site reported to confer extreme TTX resistance (Geffeney et al. 2005)

****Site reported to confer SCN4A BTX resistance (Wang & Wang, 1998)

TSR Position/Gene	SCN1A	SCN2A	SCN3A	SCN4A	SCN8A	SCN9A	SCN10A	SCN11A
P1	NA	NA	NA	*E. reginae, E. epinephelus* indenpendent origin	NA	All *E. reginae*. In *E. epinephelus* only in one individual	NA	NA
P2	NA	NA	NA	*E. reginae* independent origin	NA	NA	NA	NA
P3	NA	NA	*E. reginae* in Guaviare. *E. epinephelus* independent origin	NA	NA	All *E. reginae*	NA	NA
P4	NA	All E. epinephelus independent origin. In *E. reginae* independent origin.	*E. reginae* in Guaviare. *E. epinephelus* independent origin	NA	NA	NA	NA	NA
P5	NA	Only in one individual sample in *E. reginae* and *E. epinephelus*	Only in two few *E. epinephelus* individuals	NA	NA	NA	NA	NA
P6	NA	NA	NA	*E. aesculapii* independent origin	NA	NA	NA	*E. epinephelus* independent origin
P7	All *E. epinephelus* independent origin (AA:S). *E. reginae* only in one individual	*E. epinephelus* independent origin	*E. epinephelus* independent origin	*E. reginae, E. epinephelus, E.*sp each independent origin	NA	NA	*E. reginae* in Guaviare. *E. epinephelus* independent origin	NA
P8	All *E. epinephelus* independent origin (AA:E). *E. reginae* only in one individual	*E. epinephelus* independent origin	*E. epinephelus* independent origin	*E. reginae, E. epinephelus, E.*sp each independent origin	*E. epinephelus* in group G2 independent origin	NA	NA	NA
P9	NA	NA	NA	*E. reginae* independent origin	NA	NA	NA	NA